(1×10^7 cells) were adoptively transferred into mice by i.p. injection. One week after the transfer, the recipient mice were sacrificed and tissues were analyzed.

2.9. DC immunization

Isolation and purification of $CD11c^+$ cells from spleens from mice were performed by using CD11c MicroBeads (Miltenyi Biotec). $CD11c^+$ cells were then pulsed with HCV $NS3_{1629-1637}$ peptide for 5 h, washed with RPMI-1640 medium three times, and injected into recipient mice via footpads (2×10^5 cells). Two weeks after the transfer, spleen cells were isolated from the recipient mice and examined by the ELISPOT assay.

2.10. Statistics

Statistical significance ($P < 0.05$) was determined by 2-tailed Student's t test or ANOVA followed by Ryan's test.

3. Results

3.1. Immunization of C57BL/6 mice with DNA vaccine induces strong HCV-specific cellular immune responses

To analyze the cellular immune responses induced by the DNA vaccine, C57BL/6 mice were immunized twice with the DNA vaccine at a 2-week interval. Strong cellular immune responses to several HCV structural and non-structural proteins characterized by IFN-γ production (Fig. 2A) and cytotoxicity (Fig. 2B) were observed in CN2 or N25 DNA vaccine-immunized mice but not in mice injected with the empty plasmid DNA. We next assessed the activity of $CD8^+$ and $CD4^+$ T cells in mice immunized with the DNA vaccine. Purified $CD8^+$ or $CD4^+$ T cells from the spleen were re-stimulated in vitro with syngenic splenocytes infected with an rVV carrying the cDNA of HCV Core-NS2. Significant IFN-γ production in $CD8^+$ and $CD4^+$ T cells was observed in CN2 and N25 DNA-immunized mice but not in mice injected with the empty plasmid DNA, and the responses of $CD8^+$ T cells were much stronger than those of $CD4^+$ T cells (Fig. 2C).

3.2. Immunization with N25 DNA vaccine showed therapeutic effects in the liver of HCV transgenic mouse

We next assessed the expression of HCV protein in the liver after immunization with DNA vaccine using HCV-Tg mice. Three months after induction of HCV protein by poly(I)·poly(C) injection, $CN2\text{-}29^{(+/-)}/MxCre^{(+/-)}$ mice were immunized twice with the DNA vaccine at a 2-week interval. Immunization of mice with the N25 DNA vaccine resulted in reduced expression of HCV protein in the liver of $CN2\text{-}29^{(+/-)}/MxCre^{(+/-)}$ mice compared with the expression in mice injected with the empty plasmid DNA (Fig. 3A). Pathological changes in the liver after immunization with the DNA vaccine were also examined. Pathological changes, including swelling of hepatocytes and abnormal architecture of liver cell cords were observed in both empty plasmid DNA-immunized or CN2 DNA-immunized mice. However, these pathological changes in the liver were improved by the N25 DNA vaccine (Fig. 3B). These results suggested that the N25 DNA vaccine has a potential as a therapeutic vaccine for HCV infection.

3.3. $CD8^+$ and $CD4^+$ T cells are required for the decrease of HCV protein in the liver

We next searched for effector cells having the ability to reduce the expression of HCV protein in the N25 DNA-immunized mice. Whole spleen cells, $CD8^+$ T cells and $CD4^+$ T cells were obtained from spleens of C57BL/6 mice immunized with the N25 DNA vaccine. These cells were adoptively transferred into $CN2\text{-}29^{(+/-)}/MxCre^{(+/-)}$ mice that expressed HCV proteins. The adoptive transfer of unfractionated spleen cells, $CD8^+$ T cells or $CD4^+$ T cells decreased the expression HCV protein in the liver (Fig. 4). These results indicated that both $CD8^+$ and $CD4^+$ T cells were required for the decrease of HCV protein in the liver.

3.4. Immunization of $CN2\text{-}29^{(+/-)}/MxCre^{(+/-)}$ mice with DNA vaccine failed to induce strong HCV-specific cellular immune responses

Cellular immune responses induced by the DNA vaccine in $CN2\text{-}29^{(+/-)}/MxCre^{(+/-)}$ mice were also assessed. Unlike in WT (C57BL/6) mice, cellular immune responses to several HCV structural and non-structural proteins were reduced in the N25 DNA vaccine-immunized HCV-Tg ($CN2\text{-}29^{(+/-)}/MxCre^{(+/-)}$) mice (Fig. 5A). CD4 or CD8 T cell responses to HCV antigens were abolished in the CN2 DNA vaccine-immunized HCV-Tg mice. On the other hand, the N25 DNA vaccine elicited HCV-specific CD4 and CD8 T cell responses in HCV-Tg mice. The levels of CD4 T cell responses were equivalent to those in WT mice; however, CD8 T cell responses were weak compared with those in WT mice (Fig. 5B). These reductions of cellular immune responses were also observed in another strain of HCV-Tg ($RzCN5\text{-}15^{(+/-)}/MxCre^{(+/-)}$) mice that possessed the full-length cDNA of HCV (Fig. 5C and D).

3.5. Ability of DCs to induce HCV-specific CD8 T cells in HCV transgenic mice was not impaired

In the present study, the activity of effector cells induced by the DNA vaccine was thought to be suppressed in HCV-Tg mice. To explore these inhibitory effects on HCV-specific cellular immune responses by the DNA vaccine in HCV-Tg mice, adoptive transfer of effector cells was performed. Spleen cells were isolated from C57BL/6 mice that had been immunized with the N25 DNA vaccine. When these cells were transferred into C57BL/6 or HCV-Tg mice, nearly equal levels of CTL activities were detected in the recipient mice (Fig. 6A), suggesting that immunosuppressive mechanisms of IFN-γ production by mature CTLs did not exist in HCV-Tg mice.

Dendritic cells (DCs) play a critical role in the induction of immune responses by DNA vaccination [30]. Moreover, several studies have demonstrated that HCV impaired the function of DCs [31–34]. To assess DC function in HCV-Tg mice, DCs were freshly purified from spleens of WT and HCV-Tg ($RzCN5\text{-}15^{(+/-)}/MxCre^{(+/-)}$) mice, loaded with NS3 peptide, and transferred into WT and HCV-Tg mice. Two weeks later, the functional status of CD8 T cells in the recipient mice was evaluated. DC functions to induce HCV-specific CD8 T cell responses were not different in WT and HCV-Tg mice; however, NS3-specifc CD8 T cell responses in HCV-Tg mice that had been injected with DCs of either WT or HCV-Tg mice were much weaker than those in WT mice (Fig. 6B). These results indicated that the ability of DCs to induce HCV-specific CD8 T cells in HCV-Tg mice was not impaired.

4. Discussion

It has been reported that DNA vaccines elicited strong and long-lasting humoral and cell-mediated immune responses against pathogenic agents such as HBV, HIV, tuberculosis and malaria and that they had many advantages over traditional vaccines

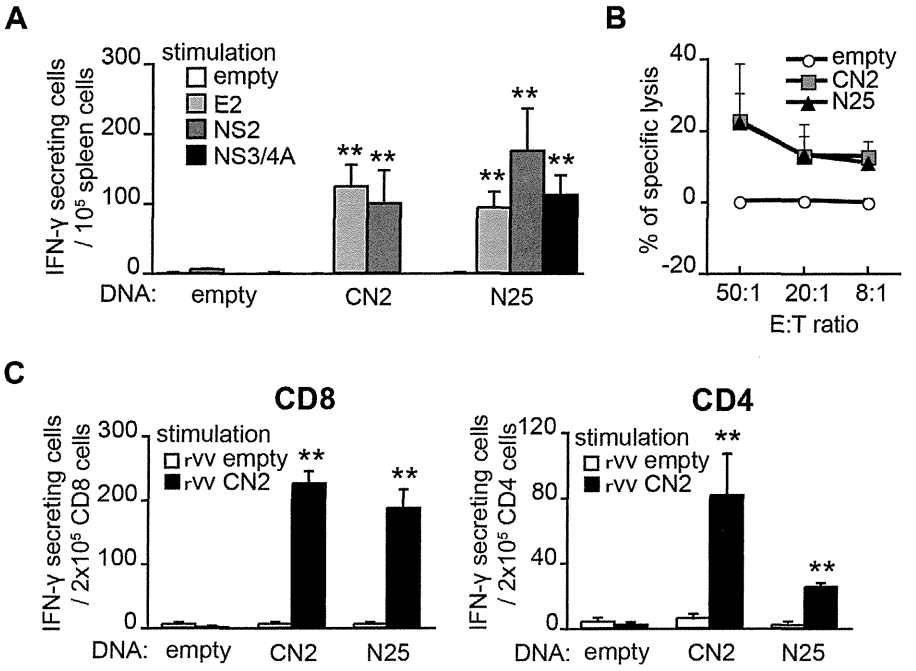

Fig. 2. Immunization of C57BL/6 mice with DNA vaccine induced strong HCV-specific cellular immune responses. C57BL/6 mice were immunized twice with the DNA vaccine at an interval of 2 weeks. At 2 weeks after the final immunization, spleen cells were isolated and examined by the IFN-γ ELISPOT assay using EL-4 cells expressing each of the HCV proteins (A), and ^{51}Cr release assay using EL-4 target cells expressing HCV NS2 protein at indicated ratios (B). CD8 and CD4 T cells were purified from whole spleen cells and examined by the IFN-γ ELISPOT assay using syngenic splenocytes infected with a recombinant vaccinia virus (rVV) carrying the cDNA of HCV Core-NS2 (rVV CN2) (C). Data are shown as means ± SEM, $n = 3$ (A and B); $n = 5$ (C). Data shown in A–C are representative of at least 3 repeated experiments. $^{**}P < 0.01$ vs stimulated with empty vector-transfected cells.

that use live-attenuated or killed pathogens, proteins, or synthetic peptides [35]. Moreover, DNA vaccine against HIV and malaria showed high levels of safety and good tolerability profile in human clinical trials [36,37]. DNA vaccines can induce cytoplasmic expression of encoded antigens (Ags) that more closely resemble native conformation of pathogens than can immunization with proteins. A DNA vaccine induced immunity against encoded Ags, whereas cytoplasmic expression using a viral vector delivery system induced immune responses to not only vaccine Ags but also vector organisms [38]. Infection with a vaccine vector virus might be an obstacle by induction of unneeded immune responses to vectors as side effects [38]. A DNA vaccine might be

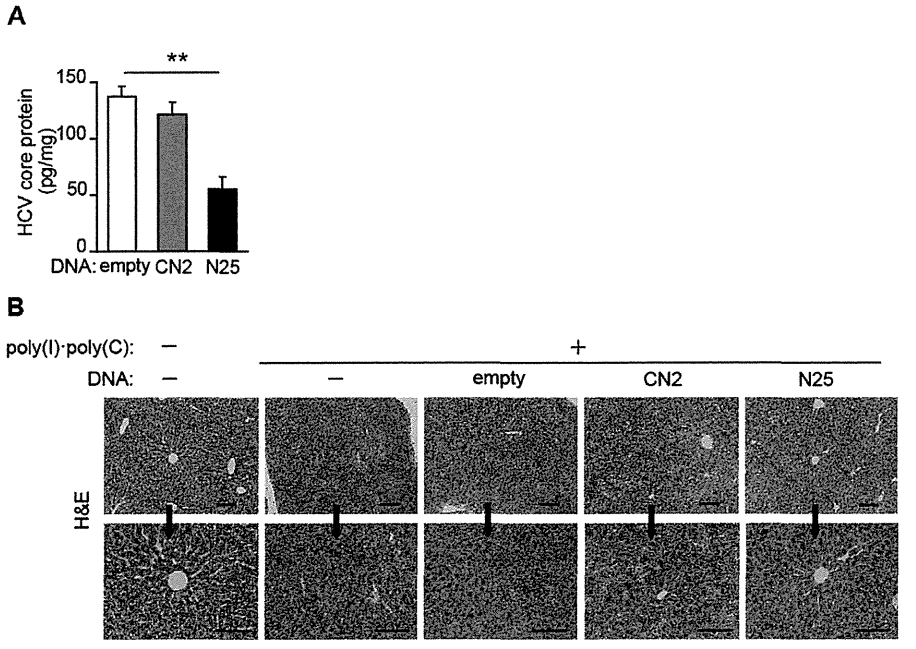

Fig. 3. Immunization with N25 DNA vaccine showed therapeutic effects in the liver of HCV transgenic mice. (A) Three months after induction of HCV protein by poly(I)·poly(C) injection, CN2-29$^{(+/-)}$/MxCre$^{(+/-)}$ mice were immunized twice with the DNA vaccine at an interval of 2 weeks. At 2 weeks after the final immunization, livers were isolated and examined for HCV core protein expression. The core protein expression in each experimental group is shown. Data are shown as means ± SEM, $n = 5$ each. $^{**}P < 0.01$. (B) Liver sections from CN2-29$^{(+/-)}$/MxCre$^{(+/-)}$ mice before (–) and after poly(I)·poly(C) injection (+). Three months after induction of HCV protein, mice were immunized three times with the DNA vaccine at intervals of 2 weeks. At 4 weeks after the final immunization, livers were isolated and stained with hematoxylin and eosin (H&E). Scale bars: 100 μm. Data shown in A and B are representative of at least 3 repeated experiments.

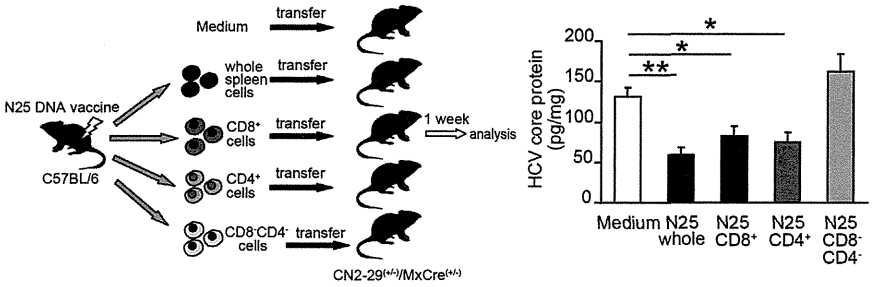

Fig. 4. $CD8^+$ and $CD4^+$ T cells are required for the decrease of HCV protein in the liver. Whole spleen cells, purified $CD8^+$ T cells or $CD4^+$ T cells from C57BL/6 mice that had been immunized twice with the N25 DNA vaccine at an interval of 2 weeks were adoptively transferred into CN2-$29^{(+/-)}$/$MxCre^{(+/-)}$ mice, and livers were isolated from the recipient mice 1 week later. The core protein expression in each experimental group is shown. Data are shown as means ± SEM, $n = 5$ each. Data are representative of 3 repeated experiments. $^{**}P < 0.01$; $^{*}P < 0.05$.

one of the best candidates for a therapeutic vaccine for infectious disease.

In the case of viral persistence resulting in chronic disease, HCV-specific CD4 and CD8 T cell responses appeared to be diminished [39]. Various hypotheses have been proposed to explain the dysfunctional T cell response in HCV infection, including viral escape mutations, exhaustion of the T cell compartment, induction of regulatory T cells and impaired DC function [40]. DCs play an important role in triggering the primary antiviral immune responses. Therefore, modulation of the function of DCs has been suggested as one of the mechanisms used by persistent viruses to evade the immune system. Several studies have demonstrated impairment of DC function in HCV-infected individuals [32,34]. On the other hand, some studies have shown that HCV proteins did not impair DC function [41–44]. In the present study, the ability of DCs to induce HCV-specific $CD8^+$ T cells in HCV transgenic mice was not impaired (Fig. 6B), therefore, another mechanism that suppressed the generation of HCV-specific CD8 T cells might exist in this mouse model.

HCV conventional transgenic mice have been used as surrogate models for chronic HCV infection in humans. In a previous study, when FVB/n Tg mice expressing HCV structural proteins (core, E1 and E2) and WT FVB/n mice were intramuscularly immunized with plasmid DNA encoding core/E1/E2, CTL activities against E2 were detected in WT mice but not in Tg mice [23], and either CD4 or CD8 T cell responses against the envelope proteins appeared to be

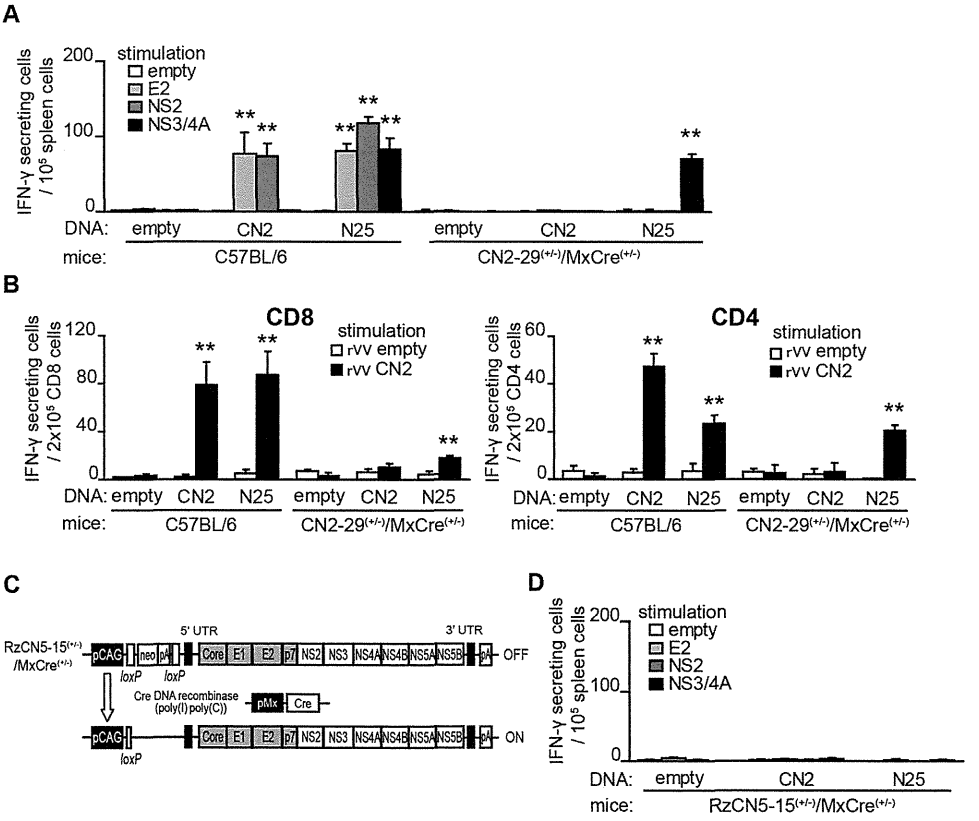

Fig. 5. Immunization of HCV-Tg mice with DNA vaccine failed to induce strong HCV-specific cellular immune responses. CN2-$29^{(+/-)}$/$MxCre^{(+/-)}$ and RzCN5-$15^{(+/-)}$/$MxCre^{(+/-)}$ mice were immunized with the DNA vaccine as in the experiment for which results are shown in Fig. 3A. (A and D) Spleen cells were isolated and examined by the IFN-γ ELISPOT assay using EL-4 cells expressing each of the HCV proteins. (B) CD8 and CD4 T cells were purified from whole spleen cells and examined by the IFN-γ ELISPOT assay using syngenic splenocytes infected with a recombinant vaccinia virus (rVV) carrying the cDNA of HCV Core-NS2 (rVV CN2). (C) HCV gene structure in RzCN5-$15^{(+/-)}$/$MxCre^{(+/-)}$ mice. RzCN5-$15^{(+/-)}$/$MxCre^{(+/-)}$ mice conditionally express full length of HCV genotype 1b cDNA. Data are shown as means ± SEM, $n = 3$ (A, B and D). Data shown in A, B and D are representative of at least 3 repeated experiments. $^{**}P < 0.01$ vs stimulated with empty vector-transfected cells.

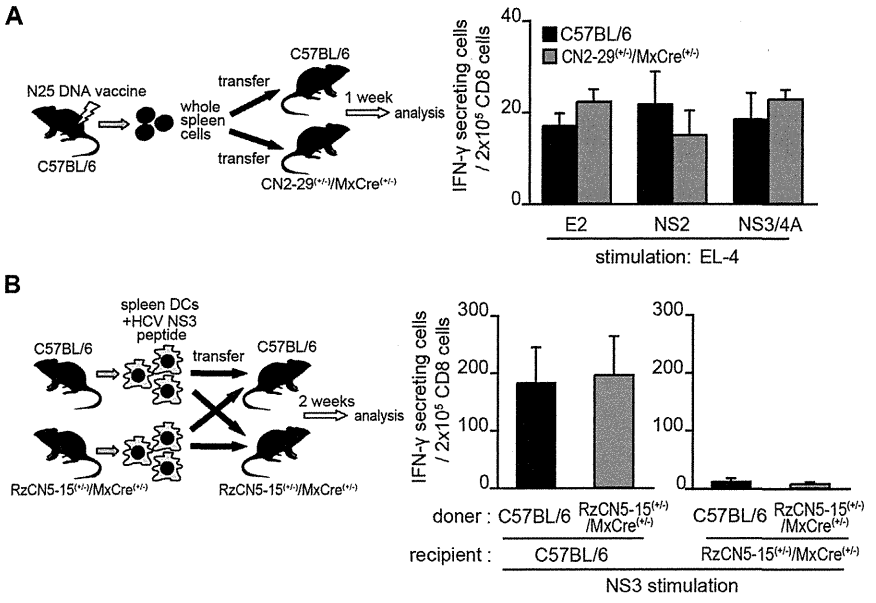

Fig. 6. Ability of DCs to induce HCV-specific CD8⁺ T cells in HCV transgenic mice was not impaired. (A) Whole spleen cells (1×10^8 cells) from C57BL/6 mice that had been immunized twice with the N25 DNA vaccine at an interval of 2 weeks were adoptively transferred into C57BL/6 or CN2-29$^{(+/-)}$/MxCre$^{(+/-)}$ mice, and spleen cells were isolated from the recipient mice 1 week later. CD8 T cells were purified from whole spleen cells and examined by the IFN-γ ELISPOT assay using EL-4 cells expressing each of the HCV proteins. (B) HCV NS3 peptide-pulsed spleen DCs (2×10^5 cells) derived from C57BL/6 or RzCN5-15$^{(+/-)}$/MxCre$^{(+/-)}$ mice were adoptively transferred to C57BL/6 or RzCN5-15$^{(+/-)}$/MxCre$^{(+/-)}$ mice. Two weeks later, spleen cells were isolated from the recipient mice. CD8 T cells were purified from whole spleen cells and examined by the IFN-γ ELISPOT assay using HCV NS3 peptide. Data are shown as means ± SEM, $n = 3$ each. Data shown in A and B are representative of at least 3 repeated experiments.

immunologically tolerant and could not overcome this tolerance by DNA immunization in the Tg mice [23]. These observation are consistent with our findings that cellular immune responses to several HCV structural and non-structural proteins were abolished in the CN2 DNA vaccine-immunized HCV-Tg (CN2-29$^{(+/-)}$/MxCre$^{(+/-)}$) mice, unlike in WT mice (Fig. 5A and B). On the other hand, the N25 DNA vaccine induced HCV-specific CD4 and CD8 T cell responses in HCV-Tg mice, and the level of CD4 T cell responses were equivalent to those in WT mice. However, the activities of CD8 T cell responses were not high compared with those in WT mice (Fig. 5B). This difference in the efficacy of CN2 and that of N25 may be caused by the difference of the expression site of HCV construct. The CN2 DNA construct contained the HCV core protein-encoding region. Several studies have demonstrated that the HCV core protein has the immunomodulatory function of suppressing host immune responses [45]. It has been reported that HCV core protein could suppress host immune responses by inhibiting antiviral CTL activity in mice infected with recombinant vaccinia virus expressing the core protein [7], and it has also been reported that Tg mice in which the HCV core protein was expressed in T cells under the control of the CD2 promoter showed significantly reduced T cell responses, including the production of IFN-γ and IL-2, compared to those in non-Tg mice [46]. The N25 DNA construct did not contain the HCV core protein-encoding region, and the N25 DNA vaccine may therefore not be susceptible to these immunosuppressive factors derived from DNA vaccine's own self.

Immunization of HCV-Tg mice with N25 DNA vaccine resulted in improvement in pathological changes in the liver. Sekiguchi et al. [27] reported that immunization with recombinant vaccinia virus strain (rVV-N25), which encoded the same non-structural HCV proteins as those encoded by N25 DNA vaccine in this study, alleviated the symptoms of pathological changes in the liver of HCV-Tg mice. They showed that TNF-α and IL-6 are responsible for the pathological symptoms in HCV-Tg mice and that immunization with rVV-N25 rapidly suppressed the inflammatory responses. The mechanism of action of N25 DNA vaccine may be similar to that of rVV-N25, though further examination is required.

In the present study, using novel HCV conditional transgenic mice to overcome the problem of immune tolerance in HCV conventional transgenic mice, the efficacy of a candidate HCV vaccine was evaluated. The use of DNA vaccines, especially the N25 DNA vaccine, expressing a non-structural protein gene resulted in reduced expression of HCV protein and improved pathological changes in the liver. Our findings may provide new avenues toward the development of an alternative approach for the treatment of individuals chronically infected with HCV, although further studies are needed.

Acknowledgments

Financial support: This work was supported by Health Science Research Grants from the Ministry of Health, Labor and Welfare of Japan and the Ministry of Education, Culture, Sports, Science and Technology of Japan. *Conflict of interest statement*: None declared.

References

[1] Alter MJ. Epidemiology of hepatitis C in the West. Semin Liver Dis 1995;15:5–14.
[2] Grakoui A, Shoukry NH, Woollard DJ, Han JH, Hanson HL, Ghrayeb J, et al. HCV persistence and immune evasion in the absence of memory T cell help. Science 2003;302:659–62.
[3] Diepolder HM, Zachoval R, Hoffmann RM, Wierenga EA, Santantonio T, Jung MC, et al. Possible mechanism involving T-lymphocyte response to non-structural protein 3 in viral clearance in acute hepatitis C virus infection. Lancet 1995;346:1006–7.
[4] Chang KM, Thimme R, Melpolder JJ, Oldach D, Pemberton J, Moorhead-Loudis J, et al. Differential CD4(+) and CD8(+) T-cell responsiveness in hepatitis C virus infection. Hepatology 2001;33:267–76.
[5] Koziel MJ, Dudley D, Wong JT, Dienstag J, Houghton M, Ralston R, et al. Intrahepatic cytotoxic T lymphocytes specific for hepatitis C virus in persons with chronic hepatitis. J Immunol 1992;149:3339–44.
[6] Rehermann B, Chang KM, McHutchison JG, Kokka R, Houghton M, Chisari FV. Quantitative analysis of the peripheral blood cytotoxic T lymphocyte response in patients with chronic hepatitis C virus infection. J Clin Invest 1996;98:1432–40.
[7] Large MK, Kittlesen DJ, Hahn YS. Suppression of host immune response by the core protein of hepatitis C virus: possible implications for hepatitis C virus persistence. J Immunol 1999;162:931–8.
[8] Koziel MJ. Cellular immune responses against hepatitis C virus. Clin Infect Dis 2005;41(Suppl. 1):S25–31.

[9] Lagging LM, Meyer K, Hoft D, Houghton M, Belshe RB, Ray R. Immune responses to plasmid DNA encoding the hepatitis C virus core protein. J Virol 1995;69:5859–63.
[10] Pancholi P, Liu Q, Tricoche N, Zhang P, Perkus ME, Prince AM. DNA prime-canarypox boost with polycistronic hepatitis C virus (HCV) genes generates potent immune responses to HCV structural and nonstructural proteins. J Infect Dis 2000;182:18–27.
[11] Youn JW, Park SH, Cho JH, Sung YC. Optimal induction of T-cell responses against hepatitis C virus E2 by antigen engineering in DNA immunization. J Virol 2003;77:11596–602.
[12] Li YP, Kang HN, Babiuk LA, Liu Q. Elicitation of strong immune responses by a DNA vaccine expressing a secreted form of hepatitis C virus envelope protein E2 in murine and porcine animal models. World J Gastroenterol 2006;12:7126–35.
[13] Lang KA, Yan J, Draghia-Akli R, Khan A, Weiner DB. Strong HCV NS3- and NS4A-specific cellular immune responses induced in mice and Rhesus macaques by a novel HCV genotype 1a/1b consensus DNA vaccine. Vaccine 2008;26:6225–31.
[14] Arashkia A, Roohvand F, Memarnejadian A, Aghasadeghi MR, Rafati S. Construction of HCV-polytope vaccine candidates harbouring immune-enhancer sequences and primary evaluation of their immunogenicity in BALB/c mice. Virus Genes 2010;40:44–52.
[15] Masalova OV, Lesnova EI, Pichugin AV, Melnikova TM, Grabovetsky VV, Petrakova NV, et al. The successful immune response against hepatitis C nonstructural protein 5A (NS5A) requires heterologous DNA/protein immunization. Vaccine 2010;28:1987–96.
[16] Encke J, zu Putlitz J, Geissler M, Wands JR. Genetic immunization generates cellular and humoral immune responses against the nonstructural proteins of the hepatitis C virus in a murine model. J Immunol 1998;161:4917–23.
[17] Arichi T, Saito T, Major ME, Belyakov IM, Shirai M, Engelhard VH, et al. Prophylactic DNA vaccine for hepatitis C virus (HCV) infection: HCV-specific cytotoxic T lymphocyte induction and protection from HCV-recombinant vaccinia infection in an HLA-A2.1 transgenic mouse model. Proc Natl Acad Sci U S A 2000;97:297–302.
[18] Frelin L, Alheim M, Chen A, Soderholm J, Rozell B, Barnfield C, et al. Low dose and gene gun immunization with a hepatitis C virus nonstructural (NS) 3 DNA-based vaccine containing NS4A inhibit NS3/4A-expressing tumors in vivo. Gene Ther 2003;10:686–99.
[19] Simon BE, Cornell KA, Clark TR, Chou S, Rosen HR, Barry RA. DNA vaccination protects mice against challenge with *Listeria monocytogenes* expressing the hepatitis C virus NS3 protein. Infect Immun 2003;71:6372–80.
[20] Ahlén G, Nystrom J, Pult I, Frelin L, Hultgren C, Sallberg M. In vivo clearance of hepatitis C virus nonstructural 3/4A-expressing hepatocytes by DNA vaccine-primed cytotoxic T lymphocytes. J Infect Dis 2005;192:2112–6.
[21] Encke J, Bernardin J, Geib J, Barbakadze G, Bujdoso R, Stremmel W. Genetic vaccination with Flt3-L and GM-CSF as adjuvants: enhancement of cellular and humoral immune responses that results in protective immunity in a murine model of hepatitis C virus infection. World J Gastroenterol 2006;12:7118–25.
[22] Lang Kuhs KA, Toporovski R, Ginsberg AA, Shedlock DJ, Weiner DB. Induction of intrahepatic HCV NS4B, NS5A and NS5B-specific cellular immune responses following peripheral immunization. PLoS ONE 2012;7:e52165.
[23] Satoi J, Murata K, Lechmann M, Manickan E, Zhang Z, Wedemeyer H, et al. Genetic immunization of wild-type and hepatitis C virus transgenic mice reveals a hierarchy of cellular immune response and tolerance induction against hepatitis C virus structural proteins. J Virol 2001;75:12121–7.
[24] Encke J, Geissler M, Stremmel W, Wands JR. DNA-based immunization breaks tolerance in a hepatitis C virus transgenic mouse model. Hum Vaccine 2006;2:78–83.
[25] Holmström F, Pasetto A, Nahr V, Brass A, Kriegs M, Hildt E, et al. A synthetic codon-optimized hepatitis C virus nonstructural 5A DNA vaccine primes polyfunctional CD8+ T cell responses in wild-type and NS5A-transgenic mice. J Immunol 2013;190:1113–24.
[26] Kimura K, Kohara M. An experimental mouse model for hepatitis C virus. Exp Anim 2011;60:93–100.
[27] Sekiguchi S, Kimura K, Chiyo T, Ohtsuki T, Tobita Y, Tokunaga Y, et al. Immunization with a recombinant vaccinia virus that encodes nonstructural proteins of the hepatitis C virus suppresses viral protein levels in mouse liver. PLoS ONE 2012;7:e51656.
[28] Niwa H, Yamamura K, Miyazaki J. Efficient selection for high-expression transfectants with a novel eukaryotic vector. Gene 1991;108:193–9.
[29] Nishimura Y, Kamei A, Uno-Furuta S, Tamaki S, Kim G, Adachi Y, et al. A single immunization with a plasmid encoding hepatitis C virus (HCV) structural proteins under the elongation factor 1-alpha promoter elicits HCV-specific cytotoxic T-lymphocytes (CTL). Vaccine 1999;18:675–80.
[30] You Z, Huang X, Hester J, Toh HC, Chen SY. Targeting dendritic cells to enhance DNA vaccine potency. Cancer Res 2001;61:3704–11.
[31] Bain C, Fatmi A, Zoulim F, Zarski JP, Trepo C, Inchauspe G. Impaired allostimulatory function of dendritic cells in chronic hepatitis C infection. Gastroenterology 2001;120:512–24.
[32] Auffermann-Gretzinger S, Keeffe EB, Levy S. Impaired dendritic cell maturation in patients with chronic, but not resolved, hepatitis C virus infection. Blood 2001;97:3171–6.
[33] Kanto T, Hayashi N, Takehara T, Tatsumi T, Kuzushita N, Ito A, et al. Impaired allostimulatory capacity of peripheral blood dendritic cells recovered from hepatitis C virus-infected individuals. J Immunol 1999;162:5584–91.
[34] Kanto T, Inoue M, Miyatake H, Sato A, Sakakibara M, Yakushijin T, et al. Reduced numbers and impaired ability of myeloid and plasmacytoid dendritic cells to polarize T helper cells in chronic hepatitis C virus infection. J Infect Dis 2004;190:1919–26.
[35] Shedlock DJ, Weiner DB. DNA vaccination: antigen presentation and the induction of immunity. J Leukoc Biol 2000;68:793–806.
[36] Kibuuka H, Kimutai R, Maboko L, Sawe F, Schunk MS, Kroidl A, et al. A phase 1/2 study of a multiclade HIV-1 DNA plasmid prime and recombinant adenovirus serotype 5 boost vaccine in HIV-Uninfected East Africans (RV 172). J Infect Dis 2010;201:600–7.
[37] Moorthy VS, Imoukhuede EB, Milligan P, Bojang K, Keating S, Kaye P, et al. A randomised, double-blind, controlled vaccine efficacy trial of DNA/MVA ME-TRAP against malaria infection in Gambian adults. PLoS Med 2004;1:e33.
[38] Donnelly JJ, Ulmer JB, Shiver JW, Liu MA. DNA vaccines. Annu Rev Immunol 1997;15:617–48.
[39] Bowen DG, Walker CM. Adaptive immune responses in acute and chronic hepatitis C virus infection. Nature 2005;436:946–52.
[40] Losikoff PT, Self AA, Gregory SH. Dendritic cells, regulatory T cells and the pathogenesis of chronic hepatitis C. Virulence 2012:3.
[41] Longman RS, Talal AH, Jacobson IM, Albert ML, Rice CM. Presence of functional dendritic cells in patients chronically infected with hepatitis C virus. Blood 2004;103:1026–9.
[42] Piccioli D, Tavarini S, Nuti S, Colombatto P, Brunetto M, Bonino F, et al. Comparable functions of plasmacytoid and monocyte-derived dendritic cells in chronic hepatitis C patients and healthy donors. J Hepatol 2005;42:61–7.
[43] Longman RS, Talal AH, Jacobson IM, Rice CM, Albert ML. Normal functional capacity in circulating myeloid and plasmacytoid dendritic cells in patients with chronic hepatitis C. J Infect Dis 2005;192:497–503.
[44] Larsson M, Babcock E, Grakoui A, Shoukry N, Lauer G, Rice C, et al. Lack of phenotypic and functional impairment in dendritic cells from chimpanzees chronically infected with hepatitis C virus. J Virol 2004;78:6151–61.
[45] Dustin LB, Rice CM. Flying under the radar: the immunobiology of hepatitis C. Annu Rev Immunol 2007;25:71–99.
[46] Soguero C, Joo M, Chianese-Bullock KA, Nguyen DT, Tung K, Hepatitis Hahn YS. C virus core protein leads to immune suppression and liver damage in a transgenic murine model. J Virol 2002;76:9345–54.

OPEN ACCESS Freely available online

PLOS | ONE

Intranasally Administered Antigen 85B Gene Vaccine in Non-Replicating Human *Parainfluenza* Type 2 Virus Vector Ameliorates Mouse Atopic Dermatitis

Hiroshi Kitagawa[1☯], Mitsuo Kawano[2☯], Keiichi Yamanaka[1☯], Masato Kakeda[1], Kenshiro Tsuda[1], Hiroyasu Inada[3], Misao Yoneda[4], Tadashi Sakaguchi[2], Akina Nigi[2], Koumei Nishimura[2], Hiroshi Komada[4], Masato Tsurudome[2], Yasuhiro Yasutomi[5], Tetsuya Nosaka[2], Hitoshi Mizutani[1]*

1 Department of Dermatology, Mie University, Graduate School of Medicine, Tsu, Mie, Japan, **2** Department of Microbiology and Molecular Genetics, Mie University, Graduate School of Medicine, Tsu, Mie, Japan, **3** Department of Pathology, Faculty of Pharmaceutical Science, Suzuka University of Medical Science, Suzuka, Mie, Japan, **4** Department of Clinical Nutrition, Graduate School of Suzuka University of Medical Science, Suzuka; Mie, Japan, **5** Laboratory of Immunoregulation and Vaccine Research, Tsukuba Primate Research Center, National Institute of Biomedical Innovation, Tsukuba, Ibaraki, Japan

Abstract

Atopic dermatitis (AD) is a refractory and recurrent inflammatory skin disease. Various factors including heredity, environmental agent, innate and acquired immunity, and skin barrier function participate in the pathogenesis of AD. T-helper (Th) 2-dominant immunological milieu has been suggested in the acute phase of AD. Antigen 85B (Ag85B) is a 30-kDa secretory protein well conserved in *Mycobacterium* species. Ag85B has strong Th1-type cytokine inducing activity, and is expected to ameliorate Th2 condition in allergic disease. To perform Ag85B function in vivo, effective and less invasive vaccination method is required. Recently, we have established a novel functional virus vector; recombinant human *parainfluenza* type 2 virus vector (rhPIV2): highly expressive, replication-deficient, and very low-pathogenic vector. In this study, we investigated the efficacy of rhPIV2 engineered to express Ag85B (rhPIV2/Ag85B) in a mouse AD model induced by repeated oxazolone (OX) challenge. Ear swelling, dermal cell infiltrations and serum IgE level were significantly suppressed in the rhPIV2/Ag85B treated mouse group accompanied with elevated IFN-γ and IL-10 mRNA expressions, and suppressed IL-4, TNF-α and MIP-2 mRNA expressions. The treated mice showed no clinical symptom of croup or systemic adverse reactions. The respiratory tract epithelium captured rhPIV2 effectively without remarkable cytotoxic effects. These results suggested that rhPIV2/Ag85B might be a potent therapeutic tool to control allergic disorders.

Citation: Kitagawa H, Kawano M, Yamanaka K, Kakeda M, Tsuda K, et al. (2013) Intranasally Administered Antigen 85B Gene Vaccine in Non-Replicating Human *Parainfluenza* Type 2 Virus Vector Ameliorates Mouse Atopic Dermatitis. PLoS ONE 8(7): e66614. doi:10.1371/journal.pone.0066614

Editor: Andreas Zirlik, University Heart Center Freiburg, Germany

Received December 31, 2012; **Accepted** May 7, 2013; **Published** July 3, 2013

Funding: K. Yamanaka (23591643) and H. Mizutani (24591647) received grants for scientific research from the Ministry of Education, Culture, Sports, Science and Technology, Japan. Other authors did not receive any financial support. The funders had no role in study design, data collection and analysis, decision to publish, or preparation of the manuscript.

Competing Interests: The authors have declared that no competing interests exist.

* E-mail: h-mizuta@clin.medic.mie-u.ac.jp

☯ These authors contributed equally to this work.

Introduction

Atopic dermatitis (AD) is a refractory and recurrent inflammatory skin disease. Heredity, environmental agent, immunity, and skin barrier function participate in the pathogenesis of AD. AD symptoms are triggered by various non-specific or specific allergic reactions. The cytokine pattern of AD, especially in the acute phase skin lesion is Th2-type cytokine dominant [1]. The barrier disrupted skin in AD is easily permitted the percutaneous entry of environmental allergens that strongly promotes Th2 immunological responses [2]. Th2 cells as well as T regulatory cell (Treg) subsets play key roles in development of AD. Patients with AD have significantly increased numbers of peripheral blood Treg compared with healthy controls, which is correlated with disease activity in AD [3,4]. This suggests involvement of some self regulation system in immune responses in AD [5].

Repeated elicitation with hapten such as oxazolone (OX) on the ear of BALB/c mice develops immediate type responses with late phase reactions followed by delayed type hypersensitivity responses. This accompanied with balance shift of cytokines in the lesional skin from Th1 to Th2 type [6], and has been utilized as mouse AD.

Ag85B is 30-kDa major secretory protein well conserved in *Mycobacterium* species [7]. The studies for the tuberculosis vaccine revealed strong activities of Ag85B in priming naïve T cells for Th1 effector cells under the appropriate conditions, and induction of strong Th1-type immune responses in mice as well as in humans [8,9]. Recently we reported that plasmid DNA vaccination encoding Ag85B derived from M. *kansasii* inhibits immediate-type hypersensitivity responses with Treg induction in skin [10], and a combined vaccination with heat-killed BCG followed by Ag85B also suppressed skin eczematous reactions in AD model mice by inducing Treg [11].

Human parainfluenza type 2 virus (hPIV2) is one of the human respiratory pathogens and a member of the genus Rubulavirus of the family Paramyxoviridae in the order Mononegavirales,

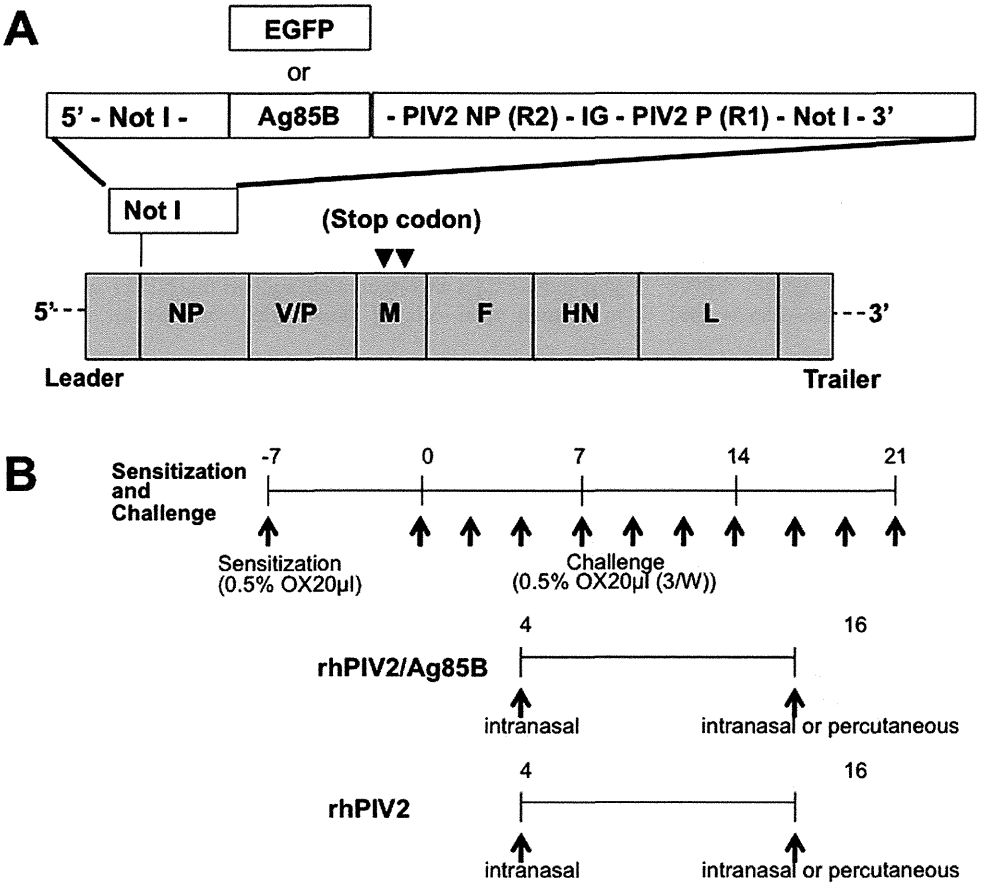

C

groups	Day4	Day16
PBS	PBS	PBS
Ag ear	rhPIV2/Ag85B	rhPIV2/Ag85B (percutaneous)
Ag nasl	rhPIV2/Ag85B	rhPIV2/Ag85B (intranasal)
PIV2 ear	rhPIV2	rhPIV2 (percutaneous)
PIV2 nasal	rhPIV2	rhPIV2 (intranasal)

Figure 1. Schematic diagram of constructs and strategy used in this study. A. The constructs of recombinant hPIV2/EGFP and hPIV2/Ag85B. The EGFP or Ag85B gene open reading frame was engineered to be flanked by hPIV2-specific gene end of NP gene (R2), intergenic sequence (IG), and gene start (R1) transcriptional signal of V/P gene. It was inserted into a cloned cDNA of the hPIV2 antigenome at a Not I site that had been engineered to be at 5′-noncoding region of NP gene. A genomic nucleotide length divisible by six (the rule of six) was maintained. For generating of replication-deficient virus, two stop codons (▼) were introduced on the M gene. **B.** Schedule for the development of a hapten-induced atopic dermatitis model and vaccination of rhPIV2/Ag85B. Mice were initially sensitized with 20 μl of 0.5% OX solution to their right ear 7 days prior to the first challenge (day -7) and then 20 μl of 0.5% OX solution was repeatedly applied on the right ear 3 times per week from day 0 until day 21. Mice were inoculated intranasally with 20 μl (5×10^6 $TCID_{50}$) of rhPIV2/Ag85B or rhPIV2 on day 4. rhPIV2 vector or phosphate buffered saline (PBS) were also applied as controls. On day 16, mice were vaccinated again intranasally or subcutaneously with PBS, rhPIV2 or rhPIV2/Ag85B. **C.** Summarized schedule of the experimental groups.
doi:10.1371/journal.pone.0066614.g001

possessing a non-segmented and negative-stranded RNA genome of 15,654 nucleotides. The genome of hPIV2 encodes 7 mRNAs [12–14] and has about 60-nt leader sequence at 3′ end and about 20-nt noncoding trailer sequence. The gene order is 3′ (leader)-NP-V/P-M-F-HN-L-(trailer)-5′. The coding proteins are the nucleocapsid (NP), the V (V) and phospho (P), the matrix (M), the fusion (F), the haemagglutinin-neuraminidase (HN), and the polymerase protein (L). The genomic RNA of the virus: viral RNA (vRNA) is encapsidated with the NP proteins, and the nucleocapsids are associated with the P and L proteins to form the

ribonucleoprotein complex. In paramyxovirus particles, vRNA is enclosed by the viral envelope composed of a cellular lipid bilayer and two envelope glycoproteins, HN and F, which are integral transmembrane proteins mediating virus attachment and cell fusion, respectively [15]. M protein underlies the lipid bilayer to ensure the structural integrity of the viral particles and is essential for interactions between the viral envelope and the RNP complex [15]. This association leads to the budding and release of viral particles from the cell surface [15].

Recently, as technology advances in reverse genetics [16], hPIVs offer several advantages as a vaccine vector. hPIVs efficiently infect the respiratory tract but don't spread far beyond it, which is an important safety factor. hPIV-based vectors have proven the effect in inducing local and systemic immunity against a number of foreign antigens [17]. hPIVs infect to various cell types and cause little cytopathic effects. Moreover, they replicate exclusively in the cytoplasm of infected cells, don't have a DNA phase during their life cycle and can thus avoid the possibility of integration of foreign genes into the host DNA genome [18].

In the present study, we utilized newly engineered rhPIV2: replication-deficient rhPIV2 vector. rhPIV2 lacks M gene that is an essential gene for virus particle formation by insertion of two stop codons. This alteration might support much safer application to animals than original proliferating virus vector. We first

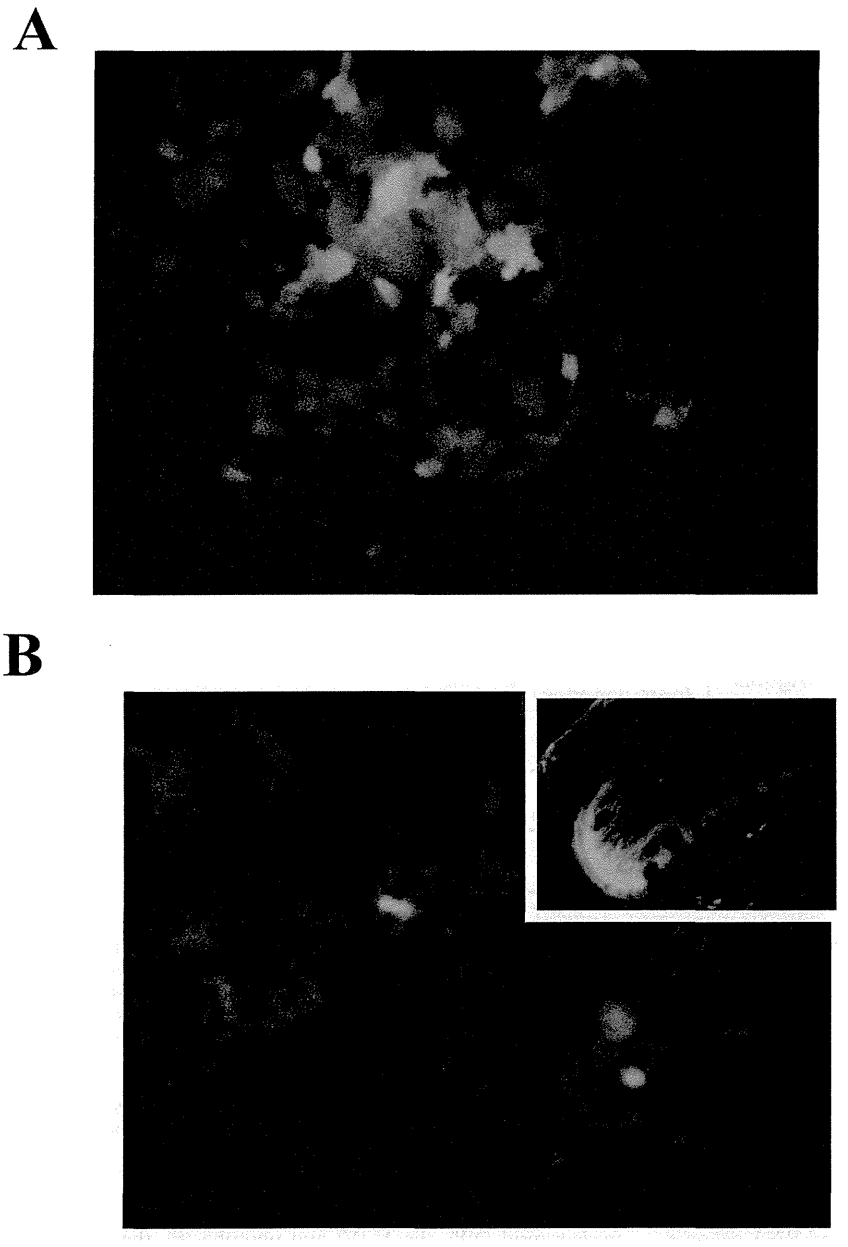

Figure 2. Expression of EGFP from rhPIV2/EGFP. A. HaCat cells were infected with rhPIV2/EGFP at an MOI of 0.5. Three days after, EGFP was clearly visualized using a fluorescence microscopy (x100). **B.** The rhPIV2/EGFP (5×10^6 $TCID_{50}$) were administered to a wild type BALB/c mice intranasally EGFP was visualized clearly in the airway epithelial cells 4 days after administration (x200, upper right box, x400).
doi:10.1371/journal.pone.0066614.g002

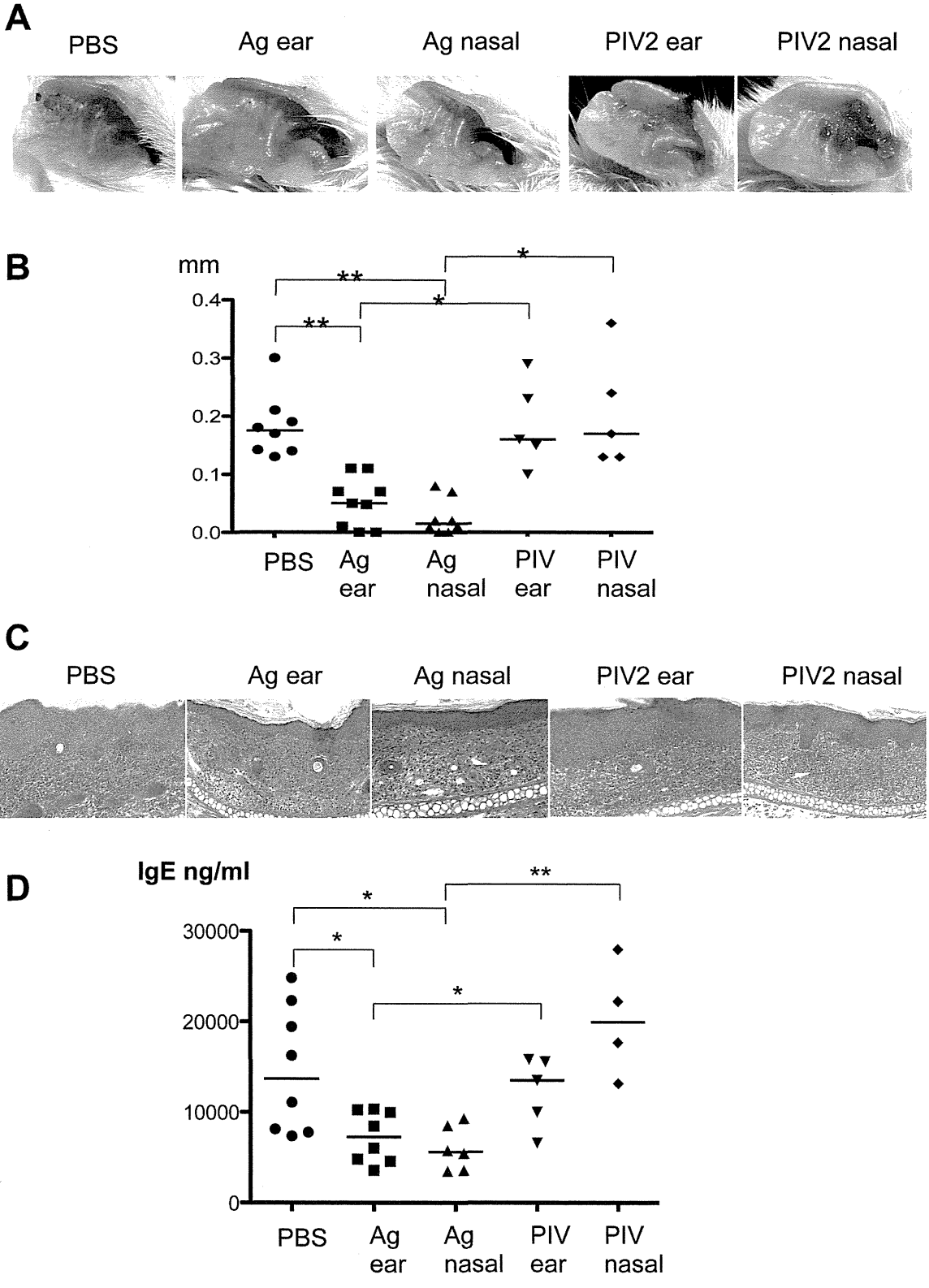

Figure 3. Anti-inflammatory effects of vaccination with rhPIV2/Ag85B. A. Clinical manifestation of the ear skin at 6 hours after OX challenge on day 21. The control groups (PBS, PIV2 ear, and PIV2 nasal on the panel) showed severe edema with erythema, however the intranasal and/or subcutaneous administration of the rhPIV2/Ag85B (Ag nasal and Ag ear on the panel, respectively) clearly reduced skin reactions in OX-sensitized mice. **B.** Ear thickness measured before and 6 hours after each OX application on day 21. The ear swelling was suppressed significantly in rhPIV2/Ag85B treated groups in two ways compared to those in the placebo treated groups. (*$P<0.05$, **$P<0.01$.) **C.** Histopathological changes of the ear skin obtained on day 21 in paraffin embedded sections stained with hematoxylin and eosin. The placebo treated groups (PBS, PIV2 ear and PIV2 nasal

on the panel) revealed marked inflammatory reactions with acanthosis and ulceration in epidermis, and marked edema with cellular infiltration including mononuclear cells and neutrophils in the dermis. The skin infiltration of inflammatory cells and epidermal thickness were decreased in rhPIV2/Ag85B treated group (Ag85B ear and Ag85B nasal on the panel). Original magnification × 100. **D.** Plasma IgE levels on day 21. Plasma IgE level was decreased in rhPIV2/Ag85B treated groups (Ag ear and Ag nasal). *P<0.05, **P<0.01.
doi:10.1371/journal.pone.0066614.g003

investigated efficiency of rhPIV2 vaccine vector expressing enhanced green fluorescence protein (EGFP) gene (rhPIV2/EGFP) in infection and expression in vitro and in vivo. Then, we evaluated effectiveness of the vaccination pathways: subcutaneous or intranasal administration of rhPIV2 expressing Ag85B gene (rhPIV2/Ag85B) in a mice AD model induced by repeated hapten challenge.

Materials and Methods

Animals

BALB/c 6-week old male mice were purchased from Japan SLC Co. (Shizuoka, Japan) and used at 7-week. Animal care was performed according to ethical guidelines, and approved by the Institutional Board Committee for Animal Care and Use of Mie University.

Construction of rhPIV2/Ag85B and rhPIV2/EGFP

rhPIV2/Ag85B and rhPIV2/EGFP was constructed according to the method reported previously, except for methods of the supply of T7 and hPIV2 RNA polymerases (NP, P, L). In brief, to generate replication-deficient rhPIV2 vector, two nucleotides change [ATG to TAG (position of 89aa) and AAG to TAG (259aa)] were introduced into the M frame of the plasmid pPIV2, a full-length cDNA copy of hPIV2 anti-genome [19] (Fig. 1A). Consequently, the 6 n length cDNA of Ag85B or EGFP, followed by transcriptional end sequence of NP gene (R2), intergenic sequence (IG), and transcriptional start signal of V/P gene (R1) ([20] was synthesized by PCR using appropriate primers), was inserted into a Not I site of the plasmid DNA encoding the replication-deficient rhPIV2 genome described above. Then, the viruses (rhPIV2/Ag85B and rhPIV2/EGFP) were recovered by co-transfection of each anti-genomic plasmid and plasmids expressing the NP, P, M and L, each cloned in a mammalian gene expression vector (pCAGGS) [21] into BSR7/5 cells expressing T7 RNA polymerase [22]. The cells were harvested, and then co-cultured with fresh Vero cells every 48 hr. Approximately 90% of the cells showed syncytia formation in the 10^{th} co-cultured cells, and its state was maintained in further co-culture. Furthermore, for virus propagation, Cos7 cells were transfected with the plasmid expressing M and co-cultured with above-mentioned 10^{th} cells. The supernatant was centrifuged at 9,000 g for 12 h at 4°C. The virus pellet was suspended in Opti-MEM (Invitrogen, Carisbad, CA, USA). The virus titers were determined by CPE method using Vero cells, and were expressed as 50% tissue culture infectious dose ($TCID_{50}$).

In vitro and in vivo Infection of rhPIV2 Vector Expressing EGFP

HaCat cells (Cell Line Service, Eppelheim, Germany) were cultured in Dulbecco's MEM supplemented with 5% (v/v) FBS, 2.0 mM L-glutamine, 100 U/ml penicillin, and 100 mg/ml streptomycin. HaCat cells were seeded one day before the transduction at 1×10^6 cells/ml (1 ml/well) in 6-well culture plates (Costar, NY, USA). The cells were incubated for 8 hours at 37°C in a 5% CO_2 atmosphere. The next day, the media was removed and 1 ml of the rhPIV2/EGFP viruses were added to the cells to be adjusted to 1×10^6 $TCID_{50}$. Two hours after infection, the media was removed and fresh culture media was supplemented to the cells. After 3 days culture, each well was observed by fluorescence microscopy.

At the next step, 20 μl of concentrated rhPIV2/EGFP (5×10^6 $TCID_{50}$) were administered into the cavity of the nose of the mice. Four days after infection, the respiratory tract and lung were sampled, embedded in Tissue-Tek OCT compound (Miles, Elkhart, USA), frozen in liquid nitrogen, and cut into 7 μm-thick sections. Sections were examined and recorded by fluorescence microscopy.

Sensitization and Challenge Schedule

Repeated hapten sensitization and challenge system was introduced in this experiment. OX (Sigma, St. Louis, MO) was dissolved in acetone/olive oil (1:1). As shown in Fig. 1B, mice were initially sensitized by pasting 20 μl of 0.5% OX solution to their right ear 7 days prior to the first challenge (day -7) and then 20 μl of 0.5% OX solution was repeatedly applied on the right ear 3 times per week from day 0 until day 21. Repeated application of OX causes delayed type hypersensitivity followed by immediate-type and late phase reaction. For vaccination, mice were infected intranasally under general anesthesia with 5×10^6 $TCID_{50}$ of the virus in a 20 μl inoculum or phosphate-buffered saline (PBS) on day 4. On day 16, mice were vaccinated again with PBS, rhPIV2/Ag85B or control rhPIV2 vector intranasally or subcutaneously to the pinna skin (Fig. 1B,C). Ear swelling was measured with thickness gauge calipers before and 6 hours after last OX challenge on day 21. Blood and pinna skins were also sampled.

Histopathological Study

The ear skins were sampled at six hours after last OX challenge on day 21. Samples were fixed in 10% neutral buffered formaldehyde and embedded in paraffin. Histological sections were of 6 mm thickness and stained with hematoxylin & eosin (H&E).

Analysis of Cytokine mRNA Expression in Mouse Ear

The mRNA was extracted from the mouse ear using Isogen (Nippon Gene, Tokyo, Japan) according to the manufacturer's instructions: One ml of homogenate was mixed with 200 μl of chloroform, and then centrifuged. The aqueous phase was separated and mixed with 0.5 ml of 2-propanol (Nacalai Tesque, Kyoto, Japan) to precipitate RNA. After centrifuging, the precipitate was washed with 70% ethanol (Nacalai Tesque) and the RNA was suspended in 40 μl of RNase-free water. The concentration of RNA was measured at 260 nm absorbent, and the quality was confirmed by electrophoresis. cDNA was synthesized from 2 μg of mRNA using an archive kit (Applied Biosystems, Foster City, CA, USA) according to the manufacturer's protocol. Real time quantitative reverse transcription-polymerase chain reaction (RT-PCR) was performed to measure transcriptional activity in skin lesions. A 25 μl reaction mixture containing 1 μg of cDNA, 900 nM of each primer, and 250 nM of TaqMan probe was mixed with 12.5 μl of TaqMan Master Mix (AB). Quantitative RT-PCR for cytokine transcripts was performed using prequalified primers and probes for IL-2, IL-4, IL-10, IL-17A, MIP2, TNF-α, TGF-β, IFN-γ and GAPDH (AB). The

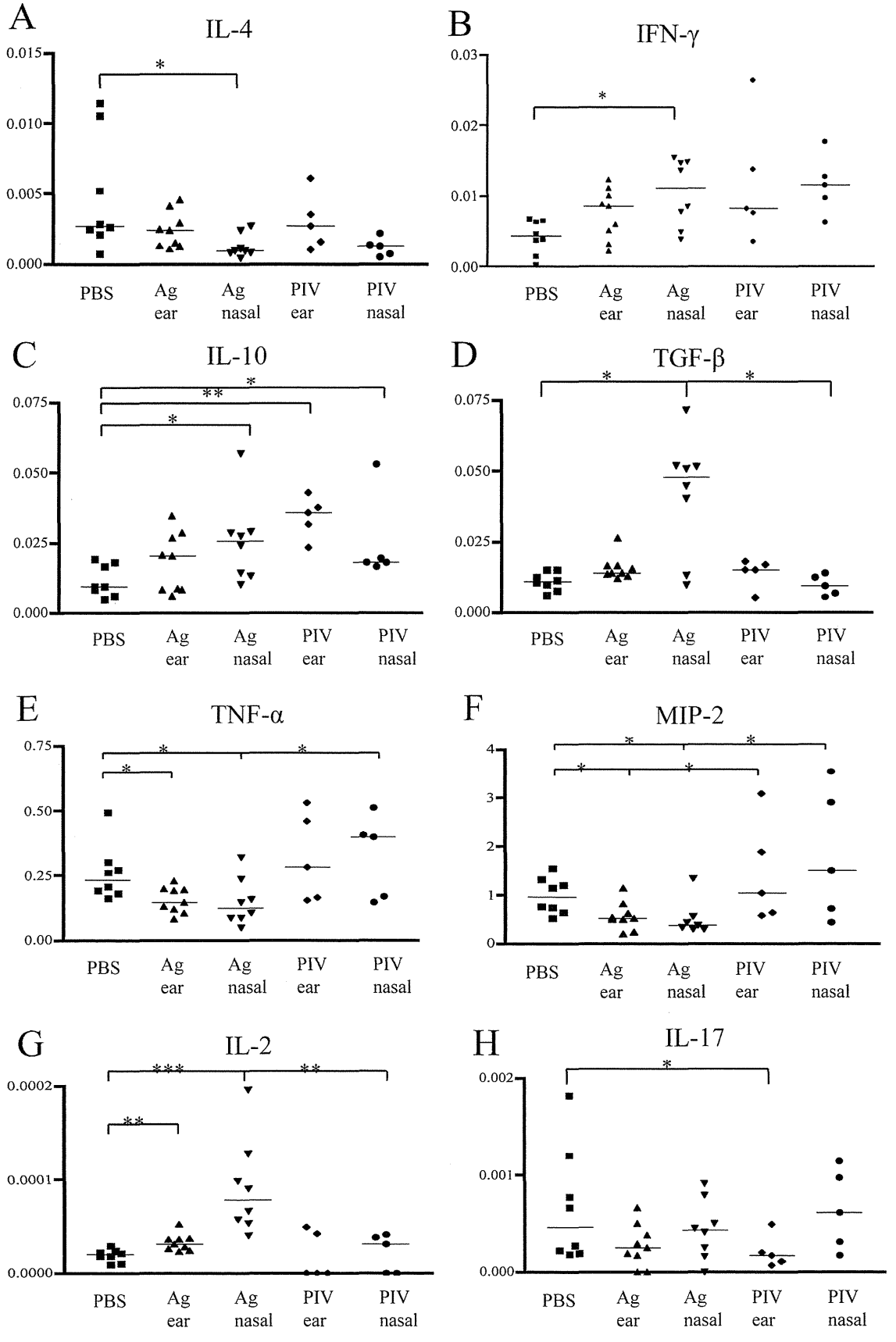
A
IL-4
0.015
0.010
0.005
0.000
*
PBS
Ag ear
Ag nasal
PIV ear
PIV nasal
B
IFN-γ
0.03
0.02
0.01
0.00
*
PBS
Ag ear
Ag nasal
PIV ear
PIV nasal
C
IL-10
0.075
0.050
0.025
0.000
*
**
*
PBS
Ag ear
Ag nasal
PIV ear
PIV nasal
D
TGF-β
0.075
0.050
0.025
0.000
*
*
PBS
Ag ear
Ag nasal
PIV ear
PIV nasal
E
TNF-α
0.75
0.50
0.25
0.00
*
*
*
PBS
Ag ear
Ag nasal
PIV ear
PIV nasal
F
MIP-2
4
3
2
1
0
*
*
*
*
PBS
Ag ear
Ag nasal
PIV ear
PIV nasal
G
IL-2
0.0002
0.0001
0.0000
***
**
**
PBS
Ag ear
Ag nasal
PIV ear
PIV nasal
H
IL-17
0.002
0.001
0.000
*
PBS
Ag ear
Ag nasal
PIV ear
PIV nasal

Figure 4. Changes in cytokines mRNA expression levels in the ears of AD mice by vaccination of rhPIV2/Ag85B. Cytokines: IL-4 (panel A), IFN-γ (panel B), IL-10 (panel C), TGF-β (panel D), TNF-α (panel E), MIP2-α (panel F), IL-2 (panel G), IL-17 (panel H), mRNA expression in the ear lesions measured with Quantitative RT-PCR. Expressions of IL-4, TNF-α and MIP2-α mRNA were significantly decreased in the ear skin treated with intra-nasally rhPIV2/Ag85B treated group compared to those of control groups. Meanwhile, the expression levels of mRNA of IFN-γ, IL-10, TGF-β and IL-2 were significantly elevated in rhPIV2/Ag85B intra-nasally treated group compared to those of control groups. *P<0.05, **P<0.01, ***P<0.001.
doi:10.1371/journal.pone.0066614.g004

ΔCt method was used to standardize the transcripts to GAPDH, and the ratio to that of control mice was calculated.

Immunohistochemistry

The ear skins sampled on day 21 were snap-frozen, and the frozen sections prepared at 7 μm thickness were subjected to a blocking procedure with 5% normal goat serum (Vector Laboratories, Burlingame, CA). Sections were then incubated with FITC-conjugated rat anti-mouse CD4 antibody (Beckman Coulter) and PE conjugated anti-mouse FoxP3 antibody (BioLegend), and examined under Fluoview FV1000 laser scanning confocal microscopy (Olympus, Tokyo, Japan). Skin infiltrating $CD4^+$ T cells and $FoxP3^+CD4^+$ T cells were counted at x100 field, and the numbers in 10 randomly chosen fields of five samples were evaluated.

Measurement of Serum IgE

Serum IgE level was determined by a sandwich enzyme-linked immunosorbent assay (Yamasa, Tokyo, Japan) according to the manufacturer's instructions. Optical density of each well was determined by using a microplate reader (Multiscan JX, Thermo Electron, Yokohama, Japan).

Statistical Analysis

Statistical analysis was performed using Mann-Whitney U-test. $P<0.05$ was considered as significant.

Results

rhPIV2/EGFP Infection in vitro and in vivo

To investigate expression levels of the inserted gene in rhPIV2 in vitro, HaCat cells were infected with rhPIV2/EGFP at an MOI of 0.5 and were examined directly using a fluorescence microscopy. The EGFP from rhPIV2/EGFP was highly expressed in HaCat cells, and remarkable fluorescence extended to nearly all the cells in spite of low MOI (Fig. 2A). Then, to evaluate the gene expression in vivo, mice were intra-nasally inoculated with rhPIV2/EGFP (5×10^6 $TCID_{50}$), and the intense EGFP expression was revealed in the lung epithelium of the mice (Fig. 2B).

Cutaneous Manifestations

To evaluate the clinically relevant therapies, mice were treated following the strategy shown in Fig. 1B. Ear lobes of the rhPIV2 (vector alone) or PBS-treated mice developed severe edematous erythema with exudation and erosion at 6 hours after OX challenge on day 21. However, rhPIV2/Ag85B-treatment reduced dermatitis in both of the intra-nasal and subcutaneous application groups (Fig. 3A). Ear swelling was dramatically suppressed in both of the rhPIV2/Ag85B-treated mice compared to PBS or rhPIV2 treated mice (Fig. 3B).

Histopathological Findings

PBS or rhPIV2-treated mice showed marked inflammatory reactions with acanthosis and ulceration in epidermis, and marked edema with cellular infiltration including mononuclear cells and neutrophils in the dermis. Both of the intra-nasal and subcutaneous rhPIV2/Ag85B application successfully reduced inflammatory cell infiltration and epidermal thickness (Fig. 3C).

Serum IgE Levels

High levels of IgE were detected in sera from PBS or rhPIV2-treated mice. On the other hand, the IgE levels in the sera from Ag85B-treated mice by two ways were suppressed significantly (Fig. 3D).

Cytokines mRNA Expression in the Ear Skins

Expression of IL-4 mRNA was significantly decreased in the ear skin of intra-nasally rhPIV2/Ag85B treatment group compared to that of PBS treated mice (Fig. 4A). In clear contrast, IFN-γ mRNA expression was significantly increased in rhPIV2/Ag85B intra-nasally treated group (Fig. 4B). As expected, IL-10 levels were significantly increased in intra-nasally treated with rhPIV2/Ag85B and rhPIV2-vector groups (Fig. 4C). Surprisingly, TGF-β expression is remarkably elevated in the intra-nasal rhPIV2/Ag85B group (Fig. 4D). mRNA expressions of TNF-α and MIP-2 were significantly decreased in both of intra-nasally and subcutaneously rhPIV2/Ag85B treated groups compared with PBS or vector treated group (Fig. 4E, F). The expression of IL-2 mRNA was also significantly elevated in both of the rhPIV2/Ag85B intra-nasally and subcutaneously treated groups (Fig. 4G). No obvious suppression in IL-17 mRNA expression was detected in rhPIV2/Ag85B group (Fig. 4H).

Immunostaining for Tregs in the Inflamed Ear Skin Lesions

As shown in Fig. 5A, $CD4^+$ T cells are displayed with green fluorescence, and $Foxp3^+$ T cells are with red. Merged yellow color means $Foxp3^+CD4^+$ T cells. The skin infiltrating $CD4^+$ T cells are significantly decreased in Ag nasal group and Ag ear group compared to that of PBS-treated group. Although it does not reach the significance, the $CD4^+$ T cells number is less in Ag nasal group compared to Ag ear group (Fig. 5B). The $Foxp3^+CD4^+$ T cells are significantly increased in both of Ag nasal and Ag ear groups (Fig. 5C).

Discussion

Immune system is finely controlled on the balance of four main subsets of Th1, Th2, Th17, and Treg [5] cells. AD, especially in its acute phase, is a disease that Th2 cells are dominantly involved in the pathogenesis. In fact PBMCs from patients with AD have increased production of IL-4, IL-5, and IL-13 with limited capacity in production of IFN-γ [23–25]. Repeated elicitation of OX on mice ear shifts the cutaneous Th1 cytokine milieu to Th2, which represents the characteristic immunological features of AD. Immunotherapy for AD has some different options to correct the imbalance of the shifted cytokine profile. In the present study, we investigated effects of vaccination using replication-deficient rhPIV2 vector expressing Ag85B gene to mouse AD model. BCG is known as a strong Th1 response modifier; however, it has a risk for granuloma formation. To avoid granuloma formation, non-wax protein antigen is required. Ag85B is a conserved protein in mycobacterial species and can elicit a strong Th1-type immune

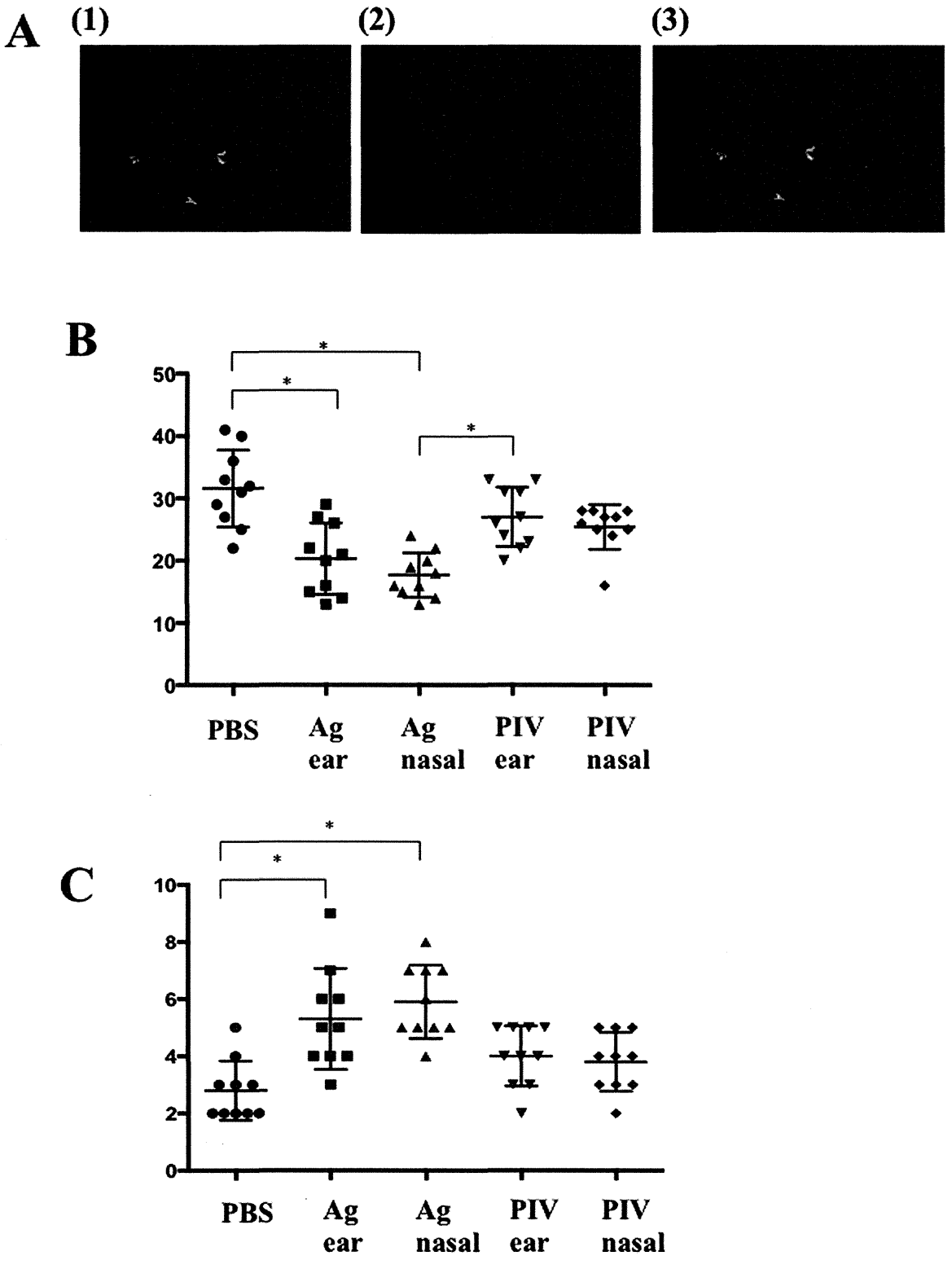

Figure 5. Immunostaining for Tregs in the inflamed ear skin lesions. A. $CD4^+$ T cells are displayed with green fluorescence (1), and $Foxp3^+$ T cells are with red (2). Merged yellow color means $Foxp3^+CD4^+$ T cells (3) (x100). **B.** The number of skin infiltrating $CD4^+$ T cells is less in Ag nasal group and Ag ear group compared to that of PBS-treated group. Although it does not reach statistical significance, $CD4^+$ T cell number is less in Ag nasal group compared to that of Ag ear group. **C.** The number of $Foxp3^+CD4^+$ T cells in the inflamed ear skin is significantly increased in both of the intra-nasal and ear-subcutaneous rhPIV2/Ag85B application groups.
doi:10.1371/journal.pone.0066614.g005

response [8]. Therefore, Ag85B has been used as immune-modulator to control acute AD lesions or asthma. Ag85B DNA vaccine suppressed airway inflammation in a murine model of asthma [26]. Furthermore, resent studies suggested that Ag85B vaccination promotes Th1-type immune responses as well as Treg responses. Administration of Ag85B showed therapeutic effects to Th2-type cytokine mediated acute phase AD models by inducing regulatory T cells [10].

Selection of the vector and its application pathway has importance in successful DNA vaccination therapy. We selected hPIV2 as a potential vector for Ag85B vaccination. hPIVs are human respiratory pathogens, and the most distinctive clinical feature of infection of hPIVs is croup (i.e., laryngotracheobronchitis or swelling around the vocal chords and other parts of the upper and middle airway). Among hPIVs, hPIV1 and hPIV3 are the major cause of croup in children, whereas hPIV2 is rarely identified as a clinical pathogen. Therefore, hPIV2 has been suspected as less virulent and cytotoxic virus. hPIV2 enters the cell by cell fusion at the plasma membrane, and replicates exclusively in the cytoplasm, and buds at the plasma membrane. Therefore, hPIV2 has no risk for integration in the host genome, not like retrovirus. In addition, since hPIV2 has a non-segmented and negative-stranded RNA genome, there is no antigenic shift among RNA segments, not like influenza viruses. Using technology of advanced reverse genetics [20], we constituted replication-deficient hPIV2 vector with additional advantage as a highly safe virus vector. To confirm the target and effective infection of rhPIV2 vector, we inoculated rhPIV2/EGFP to HaCat cells. HaCat cells successfully expressed EGFP up to 7 days post-infection (pi). Also, BALB/c mice intranasally single-administrated with rhPIV2/EGFP showed intense EGFP expression in the airway epithelial cells. These results strongly support activities of long-term high-level expression of the exogenous gene and efficiency of rhPIV2 in vivo.

In the present study, AD symptoms including ear swelling at late phase reaction were significantly suppressed in rhPIV2/Ag85B treated groups in both of intra-nasal and subcutaneous administration. Inflammatory cell infiltration including mast cells and eosinophils in the lesional skin was also suppressed. In the cytokine profile, mRNA expression of IFN-γ and IL-2 in the ear skins was significantly increased. Interestingly, IL-4 mRNA was significantly reduced in intranasal rhPIV2/Ag85B treated groups. In IL-4 suppression and IFN-γ induction, intra-nasal application showed stronger effects compared with subcutaneous application. hPIV2 is a virus infectious to the respiratory tract mucosa, and therefore more effective capture of rhPIV2/Ag85B by respiratory epithelium compared with that of skin resident cells is reasonable. In addition, the skin derived anti-infectious molecule, horny layer proteases and epithelial skin barrier might decrease efficiency of rhPIV2.

Treg induction in the effects of rhPIV2/Ag85B therapy has importance. Present study unveiled augmentation of TGF-β and IL-10 expression by intranasal rhPIV2/Ag85B. TGF-β and IL-10 have been described as critical regulatory cytokines produced by Treg. In fact in the current experiment, the numbers of skin infiltrating $CD4^+$ T cells are decreased in the nasal application and ear skin application groups accompanied with increased $FoxP3^+$ Treg population. A heat-killed Mycobacterium vaccae (*M. vaccae*) gives rise to allergen specific regulatory T cells that produce IL-10 and TGF-β, which confer the protection against airway inflammation [27]. Recently TGF-β was proved to suppress GATA-3 function through Sox4 signal, and TGF-β controls Th2 cell-mediated inflammation [28]. In addition, it is crucial that PIV2 itself has some effects in induction of Treg without obvious effects in clinical manifestation and Th1/Th2 balance.

In conclusion, the respiratory tract epithelium captured rhPIV2 effectively without remarkable cytotoxic effects. The treatment with rhPIV2/Ag85B especially by trans-nasal mucosa approach ameliorates OX-induced AD model by altering Th2/Th1 cytokine balance with induction of regulatory cytokines induction. Thus, nasal rhPIV2/Ag85B vaccination is a novel, less invasive and useful therapeutic approach for AD and related allergic disorder.

Acknowledgments

We thank Dr. K.K. Conzelmann for BSRT7/5 cells.

Author Contributions

Conceived and designed the experiments: H. Kitagawa M. Kawano. Performed the experiments: H. Kitagawa M. Kawano HI MY TS AN KN. Analyzed the data: H. Kitagawa M. Kawano. Contributed reagents/materials/analysis tools: M. Kakeda KT H. Komada MT YY. Wrote the paper: H. Kitagawa M. Kawano KY TN HM.

References

1. Grewe M, Bruijnzeel-Koomen CA, Schopf E, Thepen T, Langeveld-Wildschut AG, et al. (1998) A role for Th1 and Th2 cells in the immunopathogenesis of atopic dermatitis. Immunol Today 19: 359–361.
2. Kondo H, Ichikawa Y, Imokawa G (1998) Percutaneous sensitization with allergens through barrier-disrupted skin elicits a Th2-dominant cytokine response. Eur J Immunol 28: 769–779.
3. Ou LS, Goleva E, Hall C, Leung DY (2004) T regulatory cells in atopic dermatitis and subversion of their activity by superantigens. J Allergy Clin Immunol 113: 756–763.
4. Ito Y, Adachi Y, Makino T, Higashiyama H, Fuchizawa T, et al. (2009) Expansion of FOXP3-positive CD4+CD25+ T cells associated with disease activity in atopic dermatitis. Ann Allergy Asthma Immunol 103: 160–165.
5. Yamanaka K, Mizutani H (2011) The role of cytokines/chemokines in the pathogenesis of atopic dermatitis. Current problems in dermatology 41: 80–92.
6. Kitagaki H, Ono N, Hayakawa K, Kitazawa T, Watanabe K, et al. (1997) Repeated elicitation of contact hypersensitivity induces a shift in cutaneous cytokine milieu from a T helper cell type 1 to a T helper cell type 2 profile. J Immunol 159: 2484–2491.
7. Nagai S, Wiker HG, Harboe M, Kinomoto M (1991) Isolation and partial characterization of major protein antigens in the culture fluid of Mycobacterium tuberculosis. Infect Immun 59: 372–382.
8. Takatsu K, Kariyone A (2003) The immunogenic peptide for Th1 development. Int Immunopharmacol 3: 783–800.
9. Russo DM, Kozlova N, Lakey DL, Kernodle D (2000) Naive human T cells develop into Th1 effectors after stimulation with Mycobacterium tuberculosis-infected macrophages or recombinant Ag85 proteins. Infect Immun 68: 6826–6832.
10. Mori H, Yamanaka K, Matsuo K, Kurokawa I, Yasutomi Y, et al. (2009) Administration of Ag85B showed therapeutic effects to Th2-type cytokine-mediated acute phase atopic dermatitis by inducing regulatory T cells. Arch Dermatol Res 301: 151–157.
11. Kakeda M, Yamanaka K, Kitagawa H, Tsuda K, Akeda T, et al. Heat-killed bacillus Calmette-Guerin and Mycobacterium kansasii antigen 85B combined vaccination ameliorates dermatitis in a mouse model of atopic dermatitis by inducing regulatory T cells. Br J Dermatol 166: 953–963.
12. Kawano M, Bando H, Ohgimoto S, Okamoto K, Kondo K, et al. (1990) Complete nucleotide sequence of the matrix gene of human parainfluenza type 2 virus and expression of the M protein in bacteria. Virology 179: 857–861.
13. Kawano M, Bando H, Ohgimoto S, Kondo K, Tsurudome M, et al. (1990) Sequence of the fusion protein gene of human parainfluenza type 2 virus and its 3′ intergenic region: lack of small hydrophobic (SH) gene. Virology 178: 289–292.
14. Ohgimoto S, Bando H, Kawano M, Okamoto K, Kondo K, et al. (1990) Sequence analysis of P gene of human parainfluenza type 2 virus: P and cysteine-rich proteins are translated by two mRNAs that differ by two nontemplated G residues. Virology 177: 116–123.
15. Lamb RA, Kolakofsky D (2001) Paramyxoviridae: the viruses and their replicatio. In: Knipe DM, Howley PM, editors. In Fields Virology. Fourth ed. Philadelphia: Lippincott Williams & Wilkins. 1305–1340.

16. Schnell MJ, Mebatsion T, Conzelmann KK (1994) Infectious rabies viruses from cloned cDNA. EMBO J 13: 4195–4203.
17. Bukreyev A, Lamirande EW, Buchholz UJ, Vogel LN, Elkins WR, et al. (2004) Mucosal immunisation of African green monkeys (Cercopithecus aethiops) with an attenuated parainfluenza virus expressing the SARS coronavirus spike protein for the prevention of SARS. Lancet 363: 2122–2127.
18. Tompkins SM, Lin Y, Leser GP, Kramer KA, Haas DL, et al. (2007) Recombinant parainfluenza virus 5 (PIV5) expressing the influenza A virus hemagglutinin provides immunity in mice to influenza A virus challenge. Virology 362: 139–150.
19. Kawano M, Kaito M, Kozuka Y, Komada H, Noda N, et al. (2001) Recovery of infectious human parainfluenza type 2 virus from cDNA clones and properties of the defective virus without V-specific cysteine-rich domain. Virology 284: 99–112.
20. Kawano M, Okamoto K, Bando H, Kondo K, Tsurudome M, et al. (1991) Characterizations of the human parainfluenza type 2 virus gene encoding the L protein and the intergenic sequences. Nucleic Acids Res 19: 2739–2746.
21. Niwa H, Yamamura K, Miyazaki J (1991) Efficient selection for high-expression transfectants with a novel eukaryotic vector. Gene 108: 193–199.
22. Buchholz UJ, Finke S, Conzelmann KK (1999) Generation of bovine respiratory syncytial virus (BRSV) from cDNA: BRSV NS2 is not essential for virus replication in tissue culture, and the human RSV leader region acts as a functional BRSV genome promoter. J Virol 73: 251–259.
23. Jung T, Lack G, Schauer U, Uberuck W, Renz H, et al. (1995) Decreased frequency of interferon-gamma- and interleukin-2-producing cells in patients with atopic diseases measured at the single cell level. J Allergy Clin Immunol 96: 515–527.
24. Matsuyama T, Urano K, Ohkido M, Ozawa H, Ohta A, et al. (1999) The quantitative and qualitative defect of CD4+ CD45RO+ memory-type T cells are involved in the abnormality of TH1 immunity in atopic dermatitis patients. Clin Exp Allergy 29: 687–694.
25. Reinhold U, Wehrmann W, Kukel S, Kreysel HW (1990) Evidence that defective interferon-gamma production in atopic dermatitis patients is due to intrinsic abnormalities. Clin Exp Immunol 79: 374–379.
26. Wu J, Xu J, Cai C, Gao X, Li L, et al. (2009) Ag85B DNA vaccine suppresses airway inflammation in a murine model of asthma. Respir Res 10: 51.
27. Zuany-Amorim C, Sawicka E, Manlius C, Le Moine A, Brunet LR, et al. (2002) Suppression of airway eosinophilia by killed Mycobacterium vaccae-induced allergen-specific regulatory T-cells. Nat Med 8: 625–629.
28. Kuwahara M, Yamashita M, Shinoda K, Tofukuji S, Onodera A, et al. (2012) The transcription factor Sox4 is a downstream target of signaling by the cytokine TGF-beta and suppresses T(H)2 differentiation. Nat Immunol 13: 778–786.

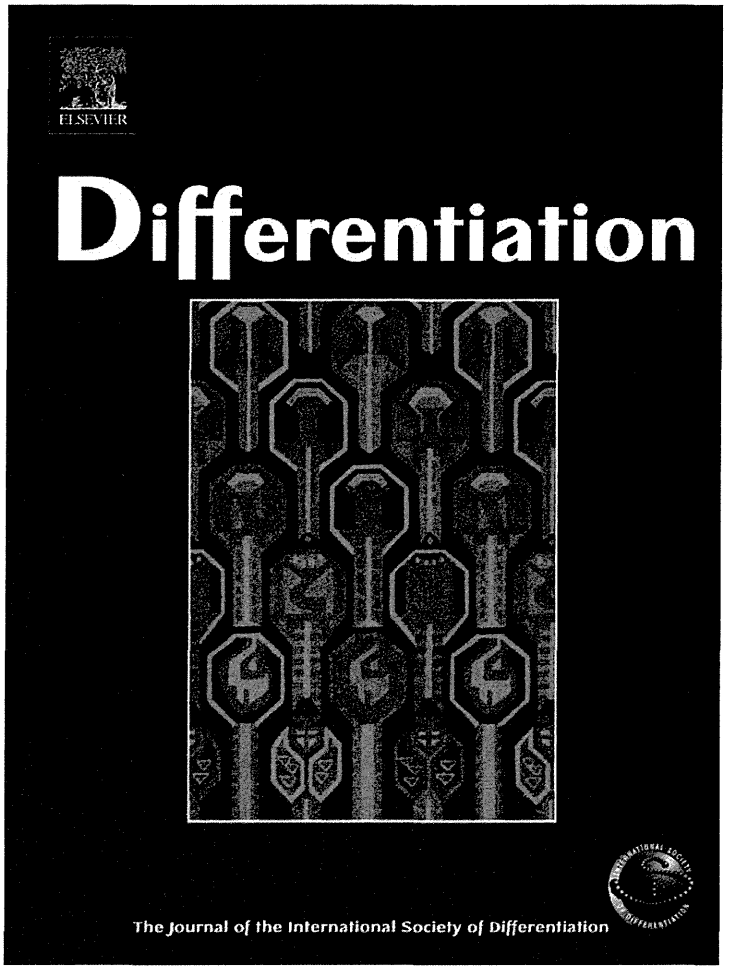

Differentiation 85 (2013) 131–139

Contents lists available at SciVerse ScienceDirect

Differentiation

journal homepage: www.elsevier.com/locate/diff

Cynomolgus monkey induced pluripotent stem cells established by using exogenous genes derived from the same monkey species

Nobuhiro Shimozawa [a,*], Ryoichi Ono [b], Manami Shimada [c], Hiroaki Shibata [a], Ichiro Takahashi [d], Hiroyasu Inada [e], Tatsuyuki Takada [c], Tetsuya Nosaka [b], Yasuhiro Yasutomi [a,f]

[a] Tsukuba Primate Research Center (TPRC), National Institute of Biomedical Innovation (NIBIO), 1-1 Hachimandai, Tsukuba, Ibaraki 305-0843, Japan
[b] Department of Microbiology and Molecular Genetics, Mie University Graduate School of Medicine, 2-174 Edobashi, Tsu, Mie 514-8507, Japan
[c] Laboratory of Cell Engineering, Department of Pharmaceutical Sciences, Ritsumeikan University, 1-1-1 Noji-higashi, Kusatsu, Shiga 525-8577, Japan
[d] Laboratory of Rare Disease Biospecimen, NIBIO, 7-6-8 Saito-Asagi, Ibaragi, Osaka 567-0085, Japan
[e] Department of Pathology, Faculty of Pharmaceutical Science, Suzuka University of Medical Science, 3500-3 Minamitamagaki-cho, Suzuka, Mie 513-8670, Japan
[f] Division of Immunoregulation, Department of Molecular and Experimental Medicine, Mie University Graduate School of Medicine, 2-174 Edobashi, Tsu, Mie 514-8507, Japan

ARTICLE INFO

Article history:
Received 28 May 2012
Received in revised form
29 January 2013
Accepted 23 February 2013

Keywords:
Induced pluripotent stem cells
Cynomolgus monkey
Cynomolgus monkey genes
Non-human primate
Medical research

ABSTRACT

Induced pluripotent stem (iPS) cells established by introduction of the transgenes POU5F1 (also known as Oct3/4), SOX2, KLF4 and c-MYC have competence similar to embryonic stem (ES) cells. iPS cells generated from cynomolgus monkey somatic cells by using genes taken from the same species would be a particularly important resource, since various biomedical investigations, including studies on the safety and efficacy of drugs, medical technology development, and research resource development, have been performed using cynomolgus monkeys. In addition, the use of xenogeneic genes would cause complicating matters such as immune responses when they are expressed. In this study, therefore, we established iPS cells by infecting cells from the fetal liver and newborn skin with amphotropic retroviral vectors containing cDNAs for the cynomolgus monkey genes of POU5F1, SOX2, KLF4 and c-MYC. Flat colonies consisting of cells with large nuclei, similar to those in other primate ES cell lines, appeared and were stably maintained. These cell lines had normal chromosome numbers, expressed pluripotency markers and formed teratomas. We thus generated cynomolgus monkey iPS cell lines without the introduction of ecotropic retroviral receptors or other additional transgenes by using the four allogeneic transgenes. This may enable detailed analysis of the mechanisms underlying the reprogramming. In conclusion, we showed that iPS cells could be derived from cynomolgus monkey somatic cells. To the best of our knowledge, this is the first report on iPS cell lines established from cynomolgus monkey somatic cells by using genes from the same species.

1. Introduction

Pluripotent stem cells that have competence similar to embryonic stem (ES) cells have been artificially generated from mouse somatic cells *in vitro* (Takahashi and Yamanaka, 2006). Establishment of this cell population, named induced pluripotent stem (iPS) cells, was achieved by introduction of the exogenous transgenes POU5F1 (also known as Oct3/4), SOX2, KLF4 and c-MYC using retroviral vectors. The iPS cell lines showed the characteristic morphologies and protein and gene expressions, as well as the karyotype stability and differentiation ability, of ES cells. It was also confirmed that mouse iPS cells differentiated into functional germ cells in the chimera gonads (Okita et al., 2007). Furthermore, iPS cells were successfully established from human somatic cells (Takahashi et al., 2007).

Cynomolgus monkeys (*Macaca fascicularis*) are one of the most important species of non-human primates, and are essential to biomedical research due to their close relationship to humans. In addition, cynomolgus monkeys are annual breeders, and in this respect are more similar to humans than rhesus monkeys, which are seasonal breeders. In non-human primates, the establishment of ES cell lines has been reported in the rhesus monkey (*Macaca mulatta*) (Thomson et al. 1995), the common marmoset (*Callithrix jacchus*) (Thomson et al. 1996), the cynomolgus monkey (Suemori et al., 2001) and the African green monkey (*Cercopithecus aethiops*) (Shimozawa et al., 2010). Before ES cells can be used for clinical

* Corresponding author. Tel.: +81 29 837 2121; fax: +81 29 837 0218.
E-mail address: shimo@nibio.go.jp (N. Shimozawa).

0301-4681/$ - see front matter © 2013 International Society of Differentiation. Published by Elsevier B.V. All rights reserved.
Join the International Society for Differentiation (www.isdifferentiation.org)
http://dx.doi.org/10.1016/j.diff.2013.02.004

applications in humans, research using non-human primates, especially cynomolgus monkeys, will be needed to examine their safety and efficacy.

Among non-human primates, iPS cells have been established in rhesus monkeys (Liu et al., 2008) and common marmosets (Tomioka et al., 2010) and cynomolgus monkeys (Okahara-Narita et al., 2012). Research into regenerative medicine using rhesus monkeys, common marmosets and cynomolgus monkeys is particularly active, and the differentiation of ES cells into various somatic cells is also being widely studied. Similar studies have also been performed on iPS cells. However, some abnormal characteristics of iPS cells have been reported (Kim et al., 2010; Lister et al., 2011; Nishino et al., 2011), and there is uncertainty with regard to their safety and efficacy. Therefore, the ideal induction methods for achieving fully reprogrammed pluripotent stem cells are currently under investigation (Maekawa et al., 2011).

The Tsukuba Primate Research Center (TPRC) in Japan has a specific pathogen-free (SPF) colony of cynomolgus monkeys that have been maintained by indoor breeding as a closed colony with an absence of microorganism infections (Honjo, 1985; Yasutomi, 2010). Using such monkeys, the safety and efficacy of drugs, medical technology development and research resource development can be researched. Because cynomolgus monkeys are used for various types of medical research, unexpected disadvantageous effects due to the use of genes from different species need to be excluded. Therefore, to establish iPS cells, we introduced four genes (POU5F1, SOX2, KLF4 and c-MYC) cloned from cynomolgus monkeys using the amphotropic retroviral vectors produced from Plat-A cells into the somatic cells of the cynomolgus monkeys. To the best of our knowledge, this is the first report on the establishment of cynomolgus monkey iPS cell lines using genes from the monkeys themselves.

2. Materials and methods

2.1. Animals

The cynomolgus monkeys (*Macaca fascicularis*) used in this study were bred and maintained in an air-conditioned room at the TPRC with controlled illumination (12 h light/12 h dark), temperature (25±2 °C), humidity (60±5%), and ventilation (10 cycles/h), and were given 70 g of commercial food (Type AS; Oriental Yeast Co., Ltd., Tokyo, Japan) and 100 g of apples daily, and unlimited access to tap water (Tsuchida et al., 2008). Every morning their health status (*e.g.*, viability, appetite, fur-coat appearance) was monitored. The maintenance of animals was conducted according to the rules for animal care of the TPRC at the National Institutes of Biomedical Innovation (NIBIO) for the care, use, and biohazard countermeasures of laboratory animals. All animal experiments were conducted in accordance with the guidelines for animal experiments of the NIBIO.

2.2. Cell culture

The newborn skin and fetal liver tissues utilized in this study were collected from the fetus and newborn delivered by Cesarean section for other studies. The tissues were thoroughly minced with scissors. The minced tissue pieces were cultured in Dulbecco's modified Eagle's medium (DMEM; Wako Pure Chemical Industries, Ltd., Osaka, Japan) with 10% fetal bovine serum (FBS; Wako Pure Chemical Industries) and 1% penicillin–streptomycin solution (Sigma, St. Louis, MO, USA). Primary cultures grown to confluence were digested with trypsin–EDTA solution (Sigma) and subcultured. Until culturing for the generation of iPS cells, the cells were kept in a Cell Banker (Nippon Zenyaku Kogyo Co., Ltd., Fukushima, Japan) in liquid nitrogen. Plat-A cells were maintained in DMEM with 10% FBS, 1% penicillin–streptomycin solution, 1 μg/mL puromycin (Sigma) and 10 μg/mL blasticidin S (Sigma). For 24 h before transfection, Plat-A cells were cultured in DMEM with 10% FBS and 1% penicillin–streptomycin solution. Cynomolgus monkey iPS cells were cultured on a mitomycin C-treated mouse embryonic fibroblast (MEF) cell monolayer derived from ICR mice (Charles River Japan, Kanagawa, Japan) on gelatin-coated 10 cm dishes in ES cell culture medium (ESM) consisting of DMEM/F12 (1:1) (Sigma) supplemented with 20% knockout serum replacement (KSR; Invitrogen), 1% GlutaMax (Invitrogen), 0.1 mM β-mercaptethanol (Sigma), 1% non-essential amino acids (Invitrogen), 10 ng/mL human recombinant leukemia inhibitory factor (hLIF; Millipore, Billerica, MA), 4 ng/mL human recombinant basic fibroblast growth factor (hbFGF; Wako Pure Chemical Industries) and 1% penicillin-streptomycin solution. For passaging, iPS cell colonies were treated with 0.1% collagenase (Wako Pure Chemical Industries) in DMEM and divided into small clusters with pipetting, then subcultured onto a new MEF layer.

2.3. Generation of iPS cells

We used KLF4, SOX2, POU5F1 and c-MYC genes from cynomolgus monkeys to establish the iPS cell lines. KLF4 and SOX2 were obtained from the JCRB Gene Bank (http://genebank.nibio.go.jp/). POU5F1 was derived from the cynomolgus monkey ES cell line, CMK6 (AGC Techno Glass Co., Ltd., Chiba, Japan). c-MYC was isolated from cynomolgus monkey skin fibroblast cells activated by bFGF.

Cynomolgus monkey iPS cells were generated as described by Takahashi and Yamanaka (2006) and Takahashi et al. (2007). Briefly, for retrovirus production, pMXs (Kitamura et al., 2003) containing cDNA of cynomolgus monkey POU5F1, SOX2, KLF4 and c-MYC, respectively, were transfected into Plat-A cells (Kitamura et al., 2003) after 24 h of culture using FUGENE6 Transfection Reagent (Roche, Basel, Switzerland). For confirmation of infection to the somatic cells, pMX containing cDNA of GFP was also prepared. After 24 h, the medium was exchanged for 2 mL of fresh medium. Cynomolgus monkey somatic cells from skin and liver were seeded at $1.5–5 \times 10^5$ cells in 10 cm dishes (BD Falcon, Franklin Lakes, NJ, USA). The next day, the supernatants with viruses produced from Plat-A cells were filtered by a cellulose acetate filter, respectively, and mixed. The somatic cells from skin and liver were infected with 2 mL of the virus-supernatants containing 4 μg/mL polybrene (Sigma) per 6 cm dish, respectively. After 24 h, the supernatants were exchanged with fresh medium. Seven days after infection, the cynomolgus monkey cells were recovered by trypsinization and seeded onto a mitomycin C-treated MEF cell monolayer on gelatin-coated 10 cm dishes in DMEM with 10% FBS and 1% penicillin–streptomycin solution. The next day, the medium was exchanged for ESM. The ES cell-like colonies were divided into small clusters with pipetting and passaged onto new feeder layers.

2.4. In vivo and in vitro differentiation

For pluripotency analysis, teratomas and embryoid bodies (EBs) were derived from iPS cells. Teratoma formation was accomplished as follows. The iPS cells suspended in ESM without β-mercaptethanol, hLIF and hbFGF were injected into the hind leg muscle of immunodeficient mice (NOD/SCID, Charles River, Japan). After about 8–12 weeks, the tumors were extracted from the hind legs and fixed with 4% paraformaldehyde (Sigma) in phosphate buffered solution (PBS), then embedded in paraffin and sectioned for histological analysis by hematoxylin and eosin staining. EBs were grown by floating culture of unattached iPS cell colonies in ESM without β-mercaptethanol, hLIF and hbFGF. After 2 weeks, EBs were cultured in DMEM with 10% FBS for attachment culture. The cells that had spontaneously differentiated from EBs were observed and analyzed by immunofluorescence. To

Table 1
Primer sets used in this study.

Gene	Forward	Reverse	bp
Endogenous POU5F1	GAGAACAATGAGAACCTTCAGGAGA	TTCTGGCGCCGGTTACAGAACCA	60
Endogenous SOX2	CCCCCGGCGGCAACGCA	TCGGCGCCGGGGAGATACAT	51
Endogenous KLF4	GAGCTCTCCCACATGAAGCGA	CGGAATGTACACCGGGTCCAA	51
Endogenous c-MYC	GAGGAGACATGGTGAACCAG	TCGAGGAGAGCAGAGAATCC	49
NANOG	CAGAAGGCCTCAGCACCT	GACTGTTCCAGGCCTGATTGTT	49
REX1	CGAAAACAGCTCGCAGAA	CAGCCTTCAAAGGGACAC	42
GAPDH	TGGACCTGACCTGCCGTCT	GGAAGAGTGGGTGTCGCTGT	49
Exogenous POU5F1	GACGGCATCGCAGCTTGGATACAC	TGAGAGGTCTCCAAGCCACCTT	50
Exogenous SOX2	GACGGCATCGCAGCTTGGATACAC	ATAATCCGGGTGCTCCTTCAT	47
Exogenous KLF4	GACGGCATCGCAGCTTGGATACAC	AATTGGAGAGGATAAAGTCCA	43
Exogenous c-MYC	GACGGCATCGCAGCTTGGATACAC	AGCTCGGTCACCATCTCCAGCT	50
AFP	TGCCAACTCAGTGAGGACAA	TCCAACAGGCCTGAGAAATC	356
Brachyury	ACCCAGTTCATAGCGGTGAC	CAATTGTCATGGGATTGCAG	392
GATA4	GCCTCTACATGAAGCTCCA	GGCTGTTCCAAGAGTCCTGC	401
Pax6	ACAGACACAGCCCTCACAAAC	ATCATAACTCCGCCCATTCACC	159
Cdx2	TCAGCCAGGTCCTCTGAGAA	GCCTGGAATTGCTCTGCC	169
VASA	CCAGAGGGCTGGATATTGAA	TGCAGGAACATCCTGTTGAG	206
β-Actin	TGAAGATCCTCACTGAGCGC	CTCTTCTCCAGGGAGGAGCT	148

examine the differentiation ability of the cells by reverse transcription polymerase chain reaction (RT-PCR), EBs at weeks 1, 2, 3 and 4 of floating culture were collected, respectively.

2.5. Gene expression analysis

Undifferentiated iPS cells and EBs at days 7, 14, 21 and 28 of culture were treated with RNA *later* (Ambion, Austin, TX, USA). RNA was isolated using an RNAqueous Kit (Ambion) according to the manufacturer's protocol. First-strand cDNA was primed via random hexamers and RT-PCR was performed with TaKara Ex Taq, TaKaRa PCR Thermal Cycler Dice Mini and a Thermal Cycler Dice Real Time System (TAKARA BIO INC., Shiga, Japan). The primer sets are shown in Table 1.

2.6. Immunocytochemistry

For immunofluorescence analysis, undifferentiated and differentiated cells were fixed with 4% paraformaldehyde in PBS for 20 min. Following permeabilization with 0.2% Triton X-100 (Sigma) in PBS for 10 min and blocking with 5% FBS in PBS for 30 min, cells were incubated with primary antibodies overnight at 4 °C and visualized by IgG or IgM conjugated with Alexa 488 (A11001, A21042, A11008, A1106, A21212) or 555 (A21428, A21422) (All 1:1000, Invitrogen). The primary antibodies used were as follows: Oct-3 (1:50, Becton Dickinson, 611203), Nanog (1:50, Repro CELL Inc., Tokyo, Japan, RCAB0003P), SSEA1 (sc-21702,), SSEA3 (sc-21703), SSEA4 (sc-21704), TRA-1-60 (sc021705), TRA-1-81 (sc-21706), and TRA-2-54 (sc-21707) (all 1:80, Santa Cruz Biotechnology, Inc. CA, USA) for undifferentiated cells, and Brachyury (1:50, Abcam, Cambridge, UK, ab20680), α-smooth muscle actin (1:100, R&D Systems, Minneapolis, MN, USA, MAB1420), β-tubulin III (1:50, Sigma, T8660) and FOXA2 (1:100, Millipore, AB4125) for differentiated cells. The nuclei were stained with 10 μg/mL Hoechst 33342 (Calbiochem, Darmstadt, Germany) in PBS.

2.7. Karyotyping

Karyotype analyses were performed at the International Council for Laboratory Animal Science Monitoring Center (Kanagawa, Japan).

3. Results

3.1. Generation of iPS cells

To investigate the viability of introducing transgenes into cells from newborn skin and fetal liver (Fig. 1A and B) using retroviral vectors produced from Plat-A cells, we first examined the efficiency of introduction of the GFP gene. The results showed that the percentages of cells expressing GFP among the total cells from the newborn skin and fetal liver samples were 77% and 68%, respectively, as determined by flow cytometry analysis (Fig. 1C and D), demonstrating the effectiveness of infection with retrovirus from Plat-A cells. Indeed, after about four weeks, ES cell-like colonies began to appear among cells from the fetal liver samples into which the four transgenes, POU5F1, SOX2, KLFf4 and c-MYC, had been introduced by retroviral vectors. We obtained 1 and 74 colonies from newborn skin and fetal liver, respectively (Fig. 1E and F). To clarify the characteristics of these colonies, we examined one line from newborn skin (S-1) and five lines from fetal liver (H-1 to H-5). The examined cell lines could be maintained by using the same methods as used for the primate ES cell lines and exhibited a flat colony morphology made up of cells with large nuclei (Fig. 1G and H).

3.2. Characterization of undifferentiated iPS cells

We examined the expression of undifferentiated markers and transgenes, as well as karyotypes, in the iPS cell lines. Immunofluorescence analysis revealed that these cell lines expressed Oct-3, SSEA4, TRA-2-54, TRA-1-60, TRA-1-81 and Nanog, but not SSEA1 and SSEA3 (Fig. 2), which was identical to the expression profile for the cynomolgus monkey ES cell lines. RT-PCR analysis revealed that these cell lines expressed endogenous POU5F1, SOX2, c-MYC, KLF4, Nanog and REX1, but not exogenous POU5F1, SOX2, c-MYC and KLF4, with the exception that exogenous c-MYC was expressed in the H-2 line (Fig. 3). In short, the expressions of the four transgenes introduced by retroviral vectors were almost silenced. Karyotyping analysis revealed that 82% (41/50), 86% (43/50), 78% (39/50) and 82% (41/50) of the S-1 (passage 23), H-1 (passage 28), H-4 (passage 23) and H-5 (passage 26) cell lines examined had a normal chromosome number of 40 and sex chromosomes XX (Fig. 4).

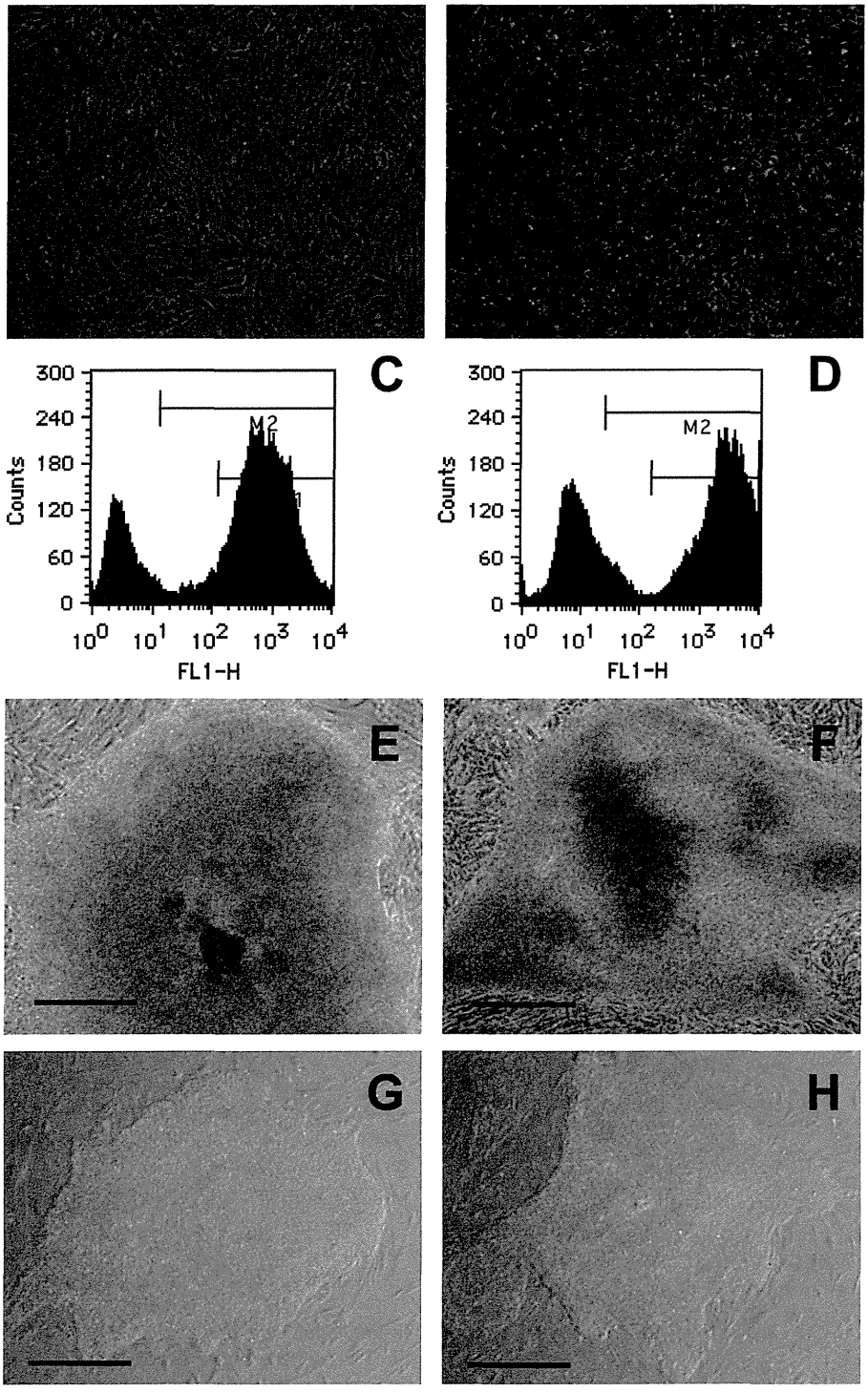

Fig. 1. Generation of iPS cell lines. The cells from newborn skin (A) and fetal liver (B) in cynomolgus monkey were cultured *in vitro*. FACS analysis revealed that, by using retroviral vectors produced from Plat-A cells, the rate of introduction of the GFP gene into both types of somatic cells was relatively high (77% and 68%, respectively) (C,D). By infection of retroviral vectors with POU5F1, SOX2, KLF4 and c-MYC into both types of somatic cells, iPS cell colonies were generated (E,F). The colonies could be maintained using the same method as for primate ES cell lines and showed flat colonies consisting of cells with large nucleoli (G,H). The bar represents 500 μm.

3.3. *Characterization of differentiated iPS cells*

We examined teratoma formation as *in vivo* differentiation, and EB formation and the expression of differentiated markers as *in vitro* differentiation. We transferred the iPS cell line into two immunodeficient mice. Four of the five transferred iPS cell lines formed, tumors, but not the H-1 line. Histological analysis revealed that the formed tumors were teratomas consisting of ectoderm, endoderm and mesoderm tissues (Fig. 5). After two weeks of the floating culture, most EBs formed solid-type clusters (Fig. 6A). EBs at 2 weeks were transferred to tissue culture dishes and outgrew. EBs spontaneously differentiated into various cell types, such as neuron-like cells, beating myocardial-like cells and pigment cells (Fig. 6B–D). Immunofluorescence analysis revealed the expression of β-tubulin III (ectoderm marker), Foxa2 (endoderm marker), and α-smooth muscle actin and Brachyury (mesoderm markers) in the